STAR: Science & Technology of Archaeological Research

ISSN: (Print) 2054-8923 (Online) Journal homepage: https://www.tandfonline.com/loi/ysta20

Soil vs. glass: an integrated approach towards the characterization of soil as a burial environment for the glassware of Cucagna Castle (Friuli, Italy)

Karl Tobias Friedrich & Patrick Degryse

To cite this article: Karl Tobias Friedrich & Patrick Degryse (2019): Soil vs. glass: an integrated approach towards the characterization of soil as a burial environment for the glassware of Cucagna Castle (Friuli, Italy), STAR: Science & Technology of Archaeological Research, DOI: 10.1080/20548923.2019.1688492

To link to this article: https://doi.org/10.1080/20548923.2019.1688492

Published online: 17 Dec 2019.

STAR: SCIENCE & TECHNOLOGY OF ARCHAEOLOGICAL RESEARCH
https://doi.org/10.1080/20548923.2019.1688492

Soil vs. glass: an integrated approach towards the characterization of soil as a burial environment for the glassware of Cucagna Castle (Friuli, Italy)

Karl Tobias Friedrich[a] and Patrick Degryse[a,b]

[a]Department of Earth and Environmental Sciences, Division of Geology, KU Leuven, Leuven, Belgium; [b]Faculty of Archaeology, Leiden University, Leiden, The Netherlands

ABSTRACT

This research is performed on a selection of archaeological glass finds with corresponding soil samples, excavated on the site of the High Medieval castle Cucagna in Friuli/Northern Italy. In the frame of understanding medieval glass technology and the chemical–physical conditions that influenced the state of preservation of the glass finds, this study uses a multi-analytical line-up of methods to characterize the composition of the glass and basic parameters of the soil including texture, mineralogical composition, pH, redox potential (Eh) and electric conductivity (EC). The results show that glass corrosion in soil not only depends on acidity, alkalinity or glass composition but also on the texture of the soil, measurable as grain-size distribution, and the mineralogical composition. The compositional groups of the glassware from Cucagna indicate the use of various raw material sources, pointing to Northern and Central Italian glass workshops with primary or secondary glass production.

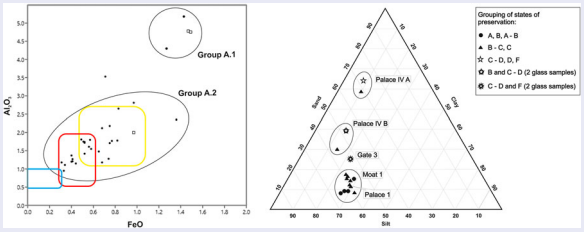

ARTICLE HISTORY
Received 5 March 2019
Accepted 18 October 2019

KEYWORDS
Soil burial environment; grain-size distribution; medieval glass; Cucagna; archaeological glass preservation

Introduction

Glassware as a group of finds in archaeological excavations of medieval sites is of particular interest because it represents multiple processes of interculturation, mainly considering the trade of ready-made tableware, the trade and use of recycled cullet for secondary glass-working, or the exploitation and trade of raw materials for primary glass production. Another aspect linked with the excavation of archaeological glass is the legal obligation to develop strategies for long-term preservation, requiring information on glass composition and the recognition of its state of preservation. Following these two main premises, the glass from the High Medieval castle Cucagna, Northern Italy, is investigated to determine locations of glass-making or glass-working and the origins of the raw materials used, to be able to deduce trade connections between the Holy Roman Empire, Venice, Milan, Tuscany and adjacent countries and regions of the Eastern Mediterranean. In the frame of a better understanding of corrosion processes in the burial environment, samples of the soil surrounding the glass fragments are characterized with respect to the chemical and physical parameters that are considered to be most relevant for affecting the deterioration processes of archaeological glass. Based upon the results of these analyses and the elemental composition of the glass fragments, a comprehensible scale system for a quick assessment of the state of preservation is developed.

The castle of Cucagna: historical background

The castle of Cucagna is situated in the rising mountain side of the Julian Alps in the very North-East of the Italian region of Friuli Venezia Giulia. It belongs to the municipality of Faedis in the Province of Udine. According to archival information, the castle was founded in 1027 by the German family of Auersberg, formerly resident in Swabia. Since at least 1161, the castle was called "cuccagna" and soon, the name of the fortress was adopted also by the family (Grönwald 2009, 179, 194). The primary purpose of this fortified castle was to secure imperial power and trading routes in Friuli, which since 952 belonged to the territory of

CONTACT Karl Tobias Friedrich karltobias.friedrich@kuleuven.be, k.tobias_friedrich@web.de Department of Earth and Environmental Sciences, Division of Geology, KU Leuven, Celestijnenlaan 200E, BE-3001 Leuven, Belgium

the Holy Roman Empire. From the early fifteenth century onwards, Cucagna lost political and strategical importance with the territorial conquest of Friuli by the Republic of Venice and was abandoned in 1522 (Grönwald 2009, 2010).

Archival evidence regarding political influence and power of the Cucagna family and its branches Zucco, Partistagno, Freschi and Valvasone is provided by only a few historic documents, showing that members of the family were repeatedly invested in offices at the court of the Patriarch of Aquileia, and even at the imperial court (Muir 1993, 183; Grönwald 2009, 194; Ludwig 2009, 113 f.). To this respect, the archaeological finds of Cucagna bear particular significance since they allow to deduce the social status of the castellans, completing the archival information with material evidence of the real-life conditions and even lifestyle of the lords with their officers and serfs. Among these finds, the fragments of glassware are of particular interest since this group of objects is generally rare in archaeological contexts and not until the Late Middle Ages also a strong indicator of financial wealth and thus, upper social classes (Felgenhauer-Schmiedt 1995, 60 f). Another important subject of research addresses the supply source for glassware: Did the lords of Cucagna receive their glassware from glasshouses in the imperial lands, e.g. from the close-by county of Carinthia, or did they purchase it on Northern Italian markets where predominantly glass from Venetian production and from other Italian glasshouses was sold.

Glass technology in Italy during the High and Late Middle Ages

The composition of glass in Medieval Europe can be divided into two main groups which roughly correspond with the geographical and historical-political situation. From the eighth century onwards glass from the Frankish (later: French and German) regions north of the Alps is characterized by the exclusive use of local raw materials, including quarry sands and ashes from beech wood or ferns. With regard to the flux components, glass from the High and Late Middle Ages contains relatively high amounts of potash (K_2O: 17.70% ± 4.62%) and lime (CaO: 18.50% ± 3.92%), with low contents of soda (Na_2O: 0.45% ± 0.41%) (average percentages, see Wedepohl 2003, 91 f., 183, 189, cf. also Wedepohl and Simon 2010).

In those regions south of the Alps towards the Eastern Mediterranean under Byzantine and Islamic patronage, another glass type became prevalent from the ninth or tenth century onwards. Due to the use of ashes from halophytic beach and desert plants from the Near East, this type of glass is characterized by relatively high amounts of sodium (Na_2O: 13.80%) with considerably lower average percentages of calcium (CaO: 8.13%) and potassium (K_2O: 2.62%) (average percentages, see Wedepohl 2003, 73 f., 177). In Northern Italy, in the High Middle Ages, the production of this Mediterranean type of alkali-silica-glass is evidenced from Liguria, e.g. the glass factories of Monte Lecco (Basso, Messiga, and Riccardi 2008) or Val Gargassa (Quartieri et al. 2005), from the Tuscan sites of Gambassi, Germagnana, Santa Cristina or Poggio Imperiale (Casellato et al. 2003; Brianese et al. 2005; Bianchin et al. 2005a, 2005b; Cagno et al. 2010; Fenzi et al. 2013) and most famously, Venice with its territories on the main land as the most extensive producer of glassware during this time (Jacoby 1993; Verità, Renier, and Zecchin 2002). From at least the thirteenth century onwards, Venetian style glass was also produced in several cities of the eastern Po-Valley and the western Adriatic coast, like Treviso, Padova, Vicenza, Mantova or Ravenna (Pause 2000, 321 f.) (see Figure 1).

In Venice, glass production is securely documented since the late tenth century in a monastic context (Gasparetto 1958, 42). The origins of a Venetian glass production for profane use are still unknown. However, in the second half of the thirteenth century, a well-developed guild of glassworkers is evidenced (Gasparetto 1958, 49). Sources from that time also reveal that there has been an intense import of Islamic (and Byzantine) glass to the city state, which was forbidden by edict in 1286 (Pause 2000, 321; referring to Monticolo 1905, 86). Excavations on the island of Torcello show the existence of secondary glassmaking from the seventh until the thirteenth century, using cullet and pieces of raw glass from other places (Verità, Renier, and Zecchin 2002, 269). The edict of 1286 seems to have fostered the production of primary glass in Venetian glasshouses. The first secure archival proof of genuine Venetian glassmaking dates to 1394, addressing an export ban of Levantine soda ash from Venice to foreign territories (Jacoby 1993, 65). This document demonstrates the awareness of Venetian glassmakers concerning the importance of using best quality raw materials for the production of colorless glass, leading to the introduction of *cristallo* in the mid of the fifteenth century. The chromatic purity of this type of glass was obtained by a very diligent selection and preparation of raw materials, including quartz pebbles from the river Ticino and purified plant ashes from Syria or Sicily (*Salsola kali* and/or *Salicornia*), both with very low iron contents (Verità 1985, 21 f., 2013). For some glass types, such as *vitrum blanchum*, an additional decolorizing effect could be achieved by carefully adding manganese to the batch. Therefore, the ratio of contents of manganese and iron must have been at least 2:1 or higher to obtain an effective decolorization (Silvestri, Molin, and Salviulo 2005, 811; Brems and Degryse 2014b, 38). Despite the attempts of Venice to control the import of Levantine ashes, smaller amounts were indeed purchased by

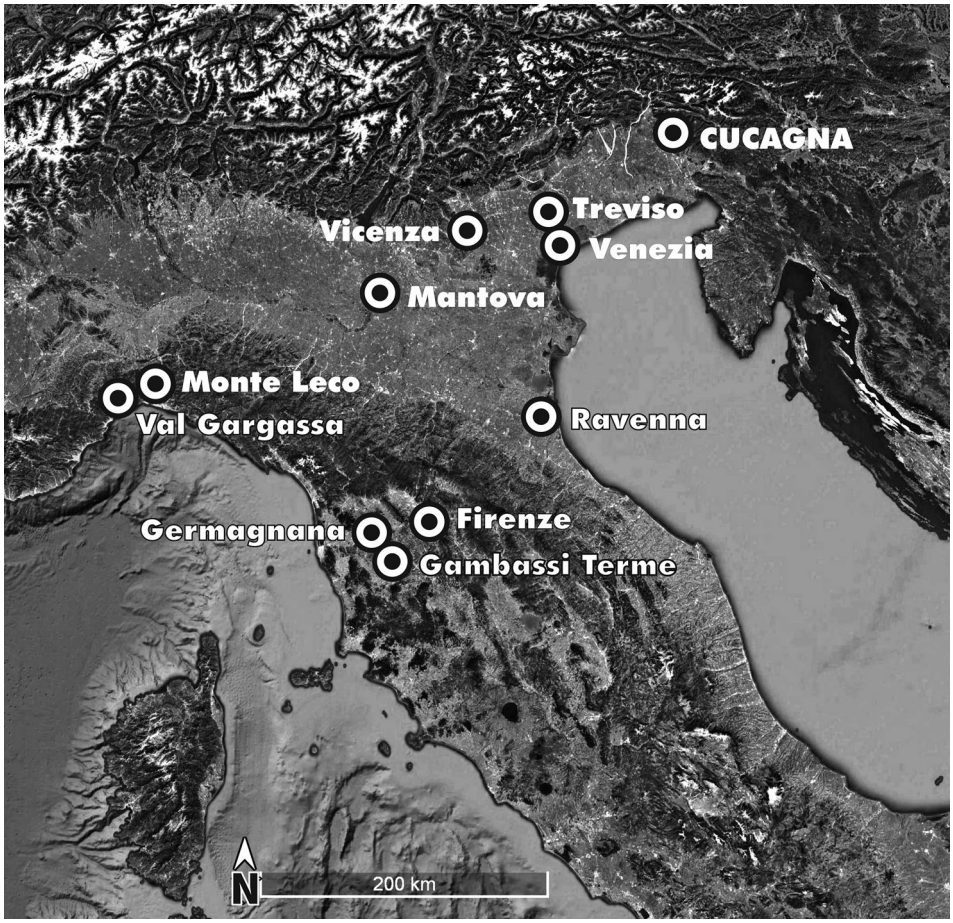

Figure 1. Satellite imagery-based map of Northern Italy with indications of the locality of the castle of Cucagna and the medieval glass factories as mentioned in this paper. © Google Earth V 7.3.2. (14 December 2015) Northern Italy. 44°02′47.88″ N, 12°39′14.77″ O, 892,59 km. Data SIO, NOAA, U.S. Navy, NGA, GEBCO, Image Landsat/Copernicus.

other glass factories in Piemonte, Liguria or Toscana (Jacoby 1993, 71). As a silica source, pebbles were also used by other Northern Italian glassmakers whereas in Tuscany local quarry sands were preferred (Jacoby 1993, 73; Casellato et al. 2003).

With respect to the complex historical-technological situation in Medieval Italy, a precise geochemical characterization of Venetian glass is difficult. To complicate the subject, the similarities in composition to contemporary Islamic glass are striking, possibly due to the continuous practice of recycling and the use of halophytic plant ashes from the Palestinian Levant (see Table 1) (Verità 2013, 522; Velde 2013, 71). However, three compositional groups of Venetian soda ash glass can be roughly distinguished: *Vitrum commune* (common glass with slight "natural" tints of yellow, blue or green, depending on the ratio of Fe(II)- and Fe(III) molecules due to specific redox conditions in the kiln atmosphere: see Silvestri, Molin, and Salviulo 2005; Zoleo et al. 2015; Bidegaray et al. 2018), *vitrum blanchum* (an almost colorless predecessor of the *cristallo* type, also made with quartz pebbles as silica source and known since at least the late thirteenth or fourteenth century), and *cristallo*. A major difference between *vitrum commune* and *vitrum blanchum* can be seen in the higher amounts of iron in the first case and a manganese content similar or slightly higher as compared to iron in the latter, resulting in ratios of manganese versus iron of 2:1 and 3:1 (Verità 1995, 89 f.,). Regarding the technological development, other criteria of distinction between the *commune*, *blanchum* and *cristallo* glass types are the decreasing amounts of alumina, magnesia and calcium, accompanied by an increase of silica and soda (Verità 2013, 527, Table 6.2.4) (see *Table 1 in this paper*).

Glass corrosion in soil burial environments

Following the chemical implications of the Random Network Theory (Zachariasen 1932; Warren 1934), it can be deduced that an acid aqueous environment accelerates the leaching of cations from the glass network, but even the mere presence of water is sufficient to leach the glass (Smets and Lommen 1982). On the other hand, alkaline conditions have a much more destructive effect, since the strong oxygen bonds of the silica tetrahedra are ruptured, leading to the breakdown of the glass structure (Molchanov and Prikhidko 1957; Böhme 1958). These predictions were confirmed by many experimental studies,

Table 1. Comparison between average compositions (and standard deviation, if available) of the three major groups of Venetian glass, extracted from Verità [1995, 90, table 3]; Biron and Verità [2012, 2708]; Verità [2013, 522; Table 6.2.4] and Wedepohl [2003], compiled from Brill [1999b].

Com-ponent	Vitrum commune (Verità 2013), mean, SD	Vitrum blanchum (Verità 1995), mean, SD	Cristallo (Biron and Verità 2012*, Verità 2013), mean, SD	Islamic glass (Brill 1999b), mean	Cucagna, mean, SD
Al_2O_3	1.64 ± 1,5	1.13 ± 0.45	< 1.0*	1.93	2.00 ± 0.98
Na_2O	12.6 ± 1.1	12.72 ± 1.18	17.2 ± 1.5	13.8	11.16 ± 1.15
K_2O	2.84 ± 0.76	2.50 ± 0.60	2.93 ± 0.41	2.67	2.55 ± 0.74
CaO	10.64 ± 0.86	10.08 ± 1.27	< 6.0*	8.13	9.64 ± 1.47
MgO	3.65 ± 0.45	3.40 ± 0.82	< 2.5*	3.44	3.42 ± 0.91
Fe_2O_3	0.74 ± 0.55	0.36 ± 0.09	< 0.3*	0.84	0.69 ± 0.31
MnO	1.00 ± 0.55	0.50 ± 0.23	0.32 ± 0.14	0.97	0.79 ± 0.46

Note: The overview shows the main glass components in their total weight percentages of the oxides, without normalization.

showing that the stability of archaeological alkali-silicate glass is clearly influenced by its chemical composition and the proton activity (expressed as $pH = -\log_{10} a\ (H^+)$) of the aqueous environment (e.g. Fletcher 1972; Melcher and Schreiner 2005; De Ferri et al. 2012; Jackson, Greenfield, and Howie 2012; De Bardi, Wiesinger, and Schreiner 2013). The gel layers of hydrated silica resulting from leaching are brittle and very sensitive to desiccation by changes of relative humidity or any kind of erosion. Thermo- or hydromechanical stress could finally lead to the loss of original substance, leaving a microscopically rough surface with spherical pits and exposed striations (Salviulo et al. 2004; Schalm et al. 2004; Genga et al. 2008; Lombardo et al. 2013). Optical-chromatic effects of this alteration are dullness, opacity, iridescence (Raman and Rajagopalan 1939) and the formation of dark brown, opaque stains within the gel layers due to redox interactions between mobilized manganese and iron (Watkinson, Weber and Anheuser 2005; Schalm et al. 2011).

In view of the complex real conditions of soil as a mixed compound system, there are far more parameters to be taken into account (Figure 2). In the first place, there is the chemical and mineralogical composition of the soil. Most obviously, seasonal (or annual, decennial, etc.) changes of weather or vegetation, as well as zoogenic or anthropogenic alterations of the soils determine the amounts of water available for chemical reactions. Consequences are changes in the concentration of dissolved inorganic and organic compounds, with implications to the redox potential (Eh) and the electrical conductivity (EC). Difficult to assess are changes of thermodynamic equilibria regarding ion exchange between the soil environment and the glass and effects of recrystallization on the microscale within the gel layers (see Pollard and Heron 2008, 179; Friedrich 2017, 92). Although the chemical properties of soil seem to be of major importance in this discussion, physical parameters should be taken into account all the same. The process of how former everyday items get in the ground to eventually become archaeological finds can be conceived as a process of sedimentation. Hence, factors like grain-size and even grain-shape play an important role in the deposit and accumulation of soil particles on the glass surface (Flemming 2007, 428 f.) (Figure 3).

The specific analytical approach chosen for this study is to implement the original soil burial environment which provided the thermodynamic matrix for glass fragments from Cucagna over the last five to seven centuries. Accordingly, the aim of this study is to evaluate the existing theories of glass deterioration in soil under approximate real conditions. In order to develop a robust analytical methodology for the characterization of the soil, some general assumptions are required:

- The most crucial reactions are taking place in the direct environment of the glass fragment, within a three-dimensional space with less than 2 cm in each direction from the surface of the glass.
- Archaeological excavation is an invasive, destructive process. Possibly existing long-term thermodynamic in-situ equilibria are inevitably disturbed by the perturbation of the soil during sampling.
- Sampling of the soil takes place at a random point in time, concerning the past and possible future burial time of the glass fragment. All measurable parameters represent chiefly the physical and chemical conditions present in this moment. In view of a standardized measurement procedure, the samples need to be dry and free of particles larger than 2 mm.

Materials and methods

Glass composition analyses

The glass finds analyzed in this study were excavated as small fragments of table ware with just a few specimens representing larger parts of vessels. The selection was carried out according to distinctive typological features, comprising free-blown and mold-blown ribbed and prunted beakers and bottles. Using the excavation stratigraphy, the glass fragments can be dated to a period from the thirteenth to the early sixteenth centuries. In total, 48 samples were taken from 41 fragments, of which seven pieces showing decorative application of blue glass threads and have therefore been sampled twice to get information about the colorless base glass and the colored glass.

The sampling was done with small precision pliers to produce samples with minimal dimensions. Following the standard procedure, the samples were embedded in transparent, colorless epoxy resin in order to obtain cross sections. After grinding and polishing, the sections were coated with a platinum/palladium film, using the Cressington 208HR sputter coater. During sample preparation, four samples were lost (sample nos. 7, 27, 45, 46). Hence, a total number of 44 samples were available for analysis.

The elemental analyses of the samples were carried out at the Università degli Studi di Pavia (UNIPV), Italy, at the Departimento di Scienze di Terra e dell'Ambiente, and at the KU Leuven, Department of Earth and Environmental Sciences. At the UNIPV, the energy-dispersive electron microprobe device FESEM Tescan MIRA XMU, equipped with an EDAX spectrometer and standardless calibration was used. The scans have been conducted using an accelerating voltage of 20 kV for the electron beam with a scanning time of 100 s each. The glass samples proved to be quite homogenous in terms of texture and inclusions with only minor compositional differences in the matrix, which allowed the calculation of average compositions from two to eight scanning points, depending on the size of the sample and the presence of transition zones between two glass types, that is, a blue thread on a colorless body (internal report: Basso 2014, cf. also Table 2).

At KUL, the measurements were carried out with the JEOL JXA-8530F HyperProbe Field Emission EPMA with five WDS spectrometers, calibrated with Corning A and validated with Corning B standards

Figure 2. View of Moat 1 (from NE to SW), with remains of outbuildings at Cucagna Castle, showing the complexity of a stratigraphy with inhomogeneous subterranean structures and different soils. © K.T. Friedrich/IRCCZ

Figure 3. Example of one of the glassware finds of Cucagna, showing the state of preservation after cleaning (left), right after excavation with *in-situ* soil agglomerations (center), and a block of the dry soil agglomerate, originally filling the hollow bottom of the beaker (right). The latter shows inhomogeneous distribution of different particle sizes or grains and the formation of small lumps and channels towards the interfacial zone between the soil and the glass. © K.T. Friedrich/IRCCZ.

(after Vicenzi et al. 2002). Prior to scanning, the sample was prepared according to the lab procedure described above, and finally coated with carbon. The scans were conducted with an acceleration voltage of 15 kV and 100 nA. The results are given as an average of five scanning spots with a diameter of 50 µm. The raw data of both measurements at UNIPV and KUL have been corrected via ZAF (for a detailed discussion on this method, see Jurek and Hulínský 1980).

Characterization of the soil

The physical and chemical soil properties chosen for characterization are:

- *Soil texture: particle-size distribution.* The distribution of particle- or grain-sizes in the soil is a basic characteristic of sediments. This physical parameter is crucial to determine the predominant grain-size class within the soil. By combining the description of the corresponding archaeological feature with the distribution of grain-sizes, basic deductions towards the potential density of the substrate and gaseous/liquid exchange processes are possible. Furthermore, the role of anthropogenic and biogenic influences of soil genesis can be better evaluated.
- *Mineralogical composition.* By detecting the crystalline phases of the soil particles, predictions on the prevalent pH and the source minerals of soluble salts of the substrate are possible. With respect to the percentage of clay minerals, and with consideration of the grain-sizes, the water retention potential can be virtually evaluated.
- *Reactive potential.* In view of the very complex interactions between the glass as a whole and its single components on one side, and the inorganic and organic minerals or compounds on the other side, the focus of this study is put firstly on the electrochemical parameters pH, redox potential (Eh),EC, and secondly, on the concentration of those water-soluble compounds which could affect the acidity/alkalinity or the buffering properties of the soil, using ICP-OES. The results of this second analysis are not part of this paper and will be presented in detail at a later stage of the study.

The sampling of the soil was carried out by the excavating archaeologists and, in some cases, by the conservator in the laboratory, meeting the above-mentioned requirements on the maximum distance from the find. Hence, 22 samples were taken, representing the direct burial environment of 23 sampled glass fragments. The soil samples derive from different locations at the site of the castle, which are described as Palazzo I, Palazzo IV A, Palazzo IV B, Gate 3 and Moat 1. After excavation, the samples were dried under atmospheric conditions. All samples are intermingled with materials of anthropogenic (grains of brick and mortar, charcoal) and biogenic origin (small roots, snail shells). Depending on the conditions of uncovering the glass fragments during excavation, the samples differ significantly in volume. Hence, the material available for analysis of at least 10 samples is limited and requires maximum efficiency. All analyses concerning the characterization of the soil were carried out at KU Leuven, Department of Earth and Environmental Science. In order to obtain as much information as possible, the following set of methods, represented here in the order of conduct, is considered to be most suitable.

Particle-size distribution

In preparation of the measurements, all samples were sieved to exclude all particles larger than 2 mm. The dry bulk was then split by pouring it for 3–4 times into a simple splitter until an effective sample amount of approx. 0.5 g was obtained. Subsequently, the samples were poured in beakers and dashed with 2 ml of demineralized water. In order to remove organic matter, 5 ml of hydrogen peroxide (H_2O_2, c: 30%) was added dropwise. The watered samples were then covered with film and kept for 2–12 h on a

Table 2. Overview of compositional inhomogeneities within one glass sample, expressed as standard deviation (SD) and its percentage of the average (% SD).

Sample no.	Measuring points	Value	Na_2O	MgO	Al_2O_3	SiO_2	P_2O_5	SO_3	Cl_2O	K_2O	CaO	TiO_2	MnO	FeO	CoO	NiO	CuO	ZnO
6	2	**mean**	11.53	3.76	1.25	68.34	0.14	0.36	1	2.46	10.20	0.05	0.54	0.4	n.d.	n.d.	n.d.	n.d.
		sd	0.01	0.03	0.03	0.23	0.02	0.05	0.02	0.02	0.03	0.05	0.02	0.03	–	–	–	–
		% SD	0.09	0.93	2.40	0.34	14.29	13.89	2	0.81	0.29	100	3.7	7.5	–	–	–	–
10	2	**mean**	13.26	3.99	1.53	66.20	0.22	0.42	0.85	2.53	9.79	0.02	0.63	0.57	n.d.	n.d.	n.d.	n.d.
		SD	0.05	0.05	0.02	0.15	0.02	0.02	0	0.02	0	0.02	0.02	0.05	–	–	–	–
		% SD	0.38	1.25	1.31	0.23	9.09	4.76	0	0.79	0	100	3.17	8.77	–	–	–	–
18	3	**mean**	10.86	4.56	1.79	67.47	n.d.	0.36	0.80	2.88	9.90	n.d.	0.91	0.47	n.d.	n.d.	n.d.	n.d.
		SD	0.02	0.06	0.01	0.07	–	0.03	0.02	0.02	0.03	–	0.10	0.06	–	–	–	–
		% SD	0.18	1.4	0.56	0.10	–	8.33	2.75	0.69	0.30	–	10.99	12.76	–	–	–	–
17	5	**mean**	10.91	4.24	1.78	66.91	0.06	0.44	0.73	2.91	9.87	0.04	0.89	0.95	n.d.	n.d.	n.d.	0.25
		SD	0.27	0.03	0.03	0.16	0.07	0.07	0.04	0.11	0.22	0.05	0.04	0.14	–	–	–	0.21
		% SD	2.47	0.71	1.68	0.23	116.67	15.91	5.48	3.78	2.23	125	4.49	14.74	–	–	–	84
39	3	**mean**	11.13	1.37	3.53	68.96	n.d.	0.32	1.04	2.24	7.84	0.2	0.97	1.43	0.19	0.15	0.21	0.37
		SD	0.09	0.02	0.02	0.14	–	0.02	0.05	0.02	0.03	0.01	0.02	0.04	0.04	0.02	0.02	0.07
		% SD	0.84	1.39	0.57	0.2	–	6.25	4.81	0.89	0.38	5	2.06	2.8	21.05	13.33	9.52	18.92
44	2	**mean**	10.94	2.75	5.07	63.74	0.63	0.17	1.08	2.34	8.42	1.74	3.22	1.40	n.d.	n.d.	n.d.	n.d.
		SD	0.02	0.03	0.02	0.20	0.11	0.09	0.03	0.04	0.06	0.01	0.03	0.02	–	–	–	–
		% SD	0.18	1.09	0.39	0.31	17.46	52.94	2.78	1.71	0.71	0.57	0.93	1.43	–	–	–	–

Note: The selection refers to those samples representing the five states of preservation (see Figure 8).

hotplate at ca. 30°C. Carbonates were not supposed to be removed. The analysis was carried out using a Beckman Coulter LS 13 320 Laser Diffraction Particle Size Analyzer, according to the procedure as follows: Rinsing of the sample container (semi-automatically); alignment of the detectors with measurement of the background (automatically); stirring of the sample and pouring it into the container; and finally, starting the measurement cycle. The generation of raw results was achieved with an included operating software, compiling an MS Excel spreadsheet.

Mineralogical characterization

The samples were weighed to achieve amounts of approx. 3 g per sample. Since the minimal amount necessary for quantification is at ca. 1 g, the measurements of sample nos. 13, 14, 15, 21 and 22 could not be quantified. The samples were then sieved and, if necessary, manually grinded to <0.5 mm. Those samples with sufficient volume for quantification were mixed with 10 wt. % of ZnO and micronized according to the lab standard, using a McCrone Micronizing Mill with 4 ml of ethanol added as grinding agent and a grinding time of 5 min (Weyns 2017). The determination of crystalline species was carried out using a Philips PW1830 X-ray diffractometer and Quanta software for computerized quantification.

Electrochemical parameters: pH, Eh, EC

The sample portions of 2 g each (abundant material) and 0.5 g (scarce material) were sieved to ≤2 mm, filled in tubes with screw caps. The samples were then dashed with demineralized water in the weight ratio 1:5 (Vranová, Marfo, and Rejšek 2015). Subsequently, the samples were shaken for one hour. For the measurements of pH and Eh, the following procedure was applied: (1) opening of all tubes to get them reacted with air and stabilized; (2) rinsing carefully the electrode, then putting it in the dispersion, stirring it with the settled material for 3 s; (3) waiting until a stable value has established, not changing for at least 15 s. Initial fluctuations during the measurement appear to often occur in diluted redox-systems. The effect might be explainable by the bias voltage of the redox electrode on the one side and the low current density of electron exchange in diluted redox systems. A standing time of approx. 10 min before reading the voltage is therefore recommended (see Böttcher and Strebel 1985, 10).

The measurements for pH and Eh were conducted with an Eijkelkamp pH 18.37. The calibration was carried out with buffer solutions for pH 4, 7, 10, using Hanna Instruments buffer solutions HI 7007 pH 7.01, HI 7004 pH 4.01 and HI 7010 pH 10.01. For the calibration of the redox electrode, the Mettler Toledo Redox Buffer solution 220 mV (pH7)/9881 was used.

For measuring the conductivity, using an Eijkelkamp EC 18.34, a similar procedure was applied. Since this took place after the pH/Eh measurements, the tubes were already open and well stabilized towards the influence of oxygen. After rinsing carefully, the electrode was put in the dispersion, stirring it within the settled soil for 3 s. A stable value was established after a few seconds.

Results and discussion

Glass composition

The glassware of Cucagna can be characterized according to the base glass composition (A) and according to color/typology (B).

(A) *Base glass composition*. The analyzed samples belong to the category of soda-silica-lime glass. With percentages of K_2O and MgO of 2.55 ± 0.74 and 3.42 ± 0.91 respectively (cf. Table 3), the use of halophytic plant ash instead of mineral soda can be assumed. Two samples of white, opaque glass show a significantly different composition with reduced silica content and high percentages of lead and tin. When renormalized to the theoretical composition of the base glass, the lead glass falls within the range of average compositions of the other samples. Hence, the glass from Cucagna can be roughly attributed to the Medieval Mediterranean type of soda-ash glass (Wedepohl 2003, 73, 103, 106).

Regarding the contents of alumina (2.00% ± 0.98%) as an impurity of the silica source, the use of both silica sands and quartz pebbles seems to have been practiced (Brems and Degryse 2014b, 32; Henderson 2000, 26). Hence, two sub-groups can be determined: group (A.1), represented in the majority of the samples, shows low to medium percentages of Al_2O_3 between 0.63% and 2.76%, indicating the use of quartz-rich pebbles with low amounts of feldspars as it was practiced by Venetian glassmakers (Jacoby 1993, 73). A second group (A.2) shows high values of alumina (3.53%–5.07%) and iron (1.25%–1.45%), pointing to the use of silica sources with relatively higher impurities of alumina and iron for primary glassmaking (see Figure 4(a)). This interpretation is substantiated by the positive correlation of Al_2O_3 vs. FeO in the biplot of Figure 4(b). Due to weathering processes of (felsic) rocks in sediment generation, silica sands can be enriched in alumina as compared to the parent rock, e.g. in the shape of clay minerals, because alumina is one of the last minerals to be depleted from the parent feldspar (Armstrong 1940, 820; Weltje and von Eynatten 2004, 4). The relatively high percentages of iron within group (A.2) could be a compositional characteristic of local sands used for primary glassmaking. In the High and Late Middle Ages, the practice of using silica sands is evidenced for e.g. Tuscan glasshouses (Casellato et al. 2003, 349 f.; Fenzi et al. 2013) and presumed for some Islamic workshops (e.g. Duckworth et al. 2015, 43).

From those major and minor components presumably deriving from the plant ash (Na_2O, CaO, K_2O, MgO and P_2O_5), two other sub-groups can be distinguished (see Figure 4(c)). Therefore, potassium is regarded as the decisive component since it marks the most conspicuous compositional difference between halophytic plants of the east and west Mediterranean (Cagno et al. 2010). The third group (A.3) shows values of K_2O between 0.79% and 2.91%, falling within tolerable ranges of Levantine ashes (Cagno et al. 2010, 3032). The fourth group (A.4), represented by only two samples, contains percentages of K_2O between 4.75% and 5.57%, whereas this group also contains the lowest Na_2O content of all Cucagna samples with 7.80%. Such high values of soda are assumed to be typical for ashes from halophytes of the western Mediterranean, like *Salsola kali* (Tite et al. 2006). The large differences in concentration of the ash components (with standard deviations between 10% and 29% as compared to the average concentration, cf. Table 3) are considered to be not unusual for plant ashes since the compositions of the halophytes depend on specific local geological conditions of growth (Barkoudah and Henderson 2006).

(B) *Color and type*. Phenomenologically, the samples can be subdivided into six chromatic-typological groups (cf. Table 4): (B.1): colorless, transparent glass (with slight hues of yellow); (B.2): naturally colored, transparent glass with hues of blue or green; (B.3): blue, transparent glass; (B.4): green, transparent glass; (B.5): brown, transparent glass; (B.6): white, opaque glass.

When compared to the compositional groups (A.1–A.4), nearly all colorless and naturally colored samples, the majority of the blue samples, one sample of a brown glass and both white opaque glasses seem to have been produced by the use of a relatively pure silica source (possibly quartz pebbles) and the Levantine type of plant ash. The blue glass no 21 is probably made with pebbles and a mixed alkali ash from elsewhere. The decolorized fragment of a bottle (no. 33), a

Table 3. Average compositions and standard deviations of the glassware from Cucagna, given in weight percent of the major and minor oxides, without normalization.

Component	Mean (wt.%)	Standard deviation
SiO_2	67.10	2.59
Al_2O3	2.00	0.98
Na_2O	11.16	1.15
CaO	9.64	1.47
MgO	3.42	0.91
K_2O	2.55	0.74
P_2O_5	0.17	0.175
FeO	0.69 (0.94)	0.31 (0.96)
MnO	0.79	0.46

Note: The table does not show the two samples containing lead as a major component. The results of iron content given in brackets refer to only those samples with blue color.

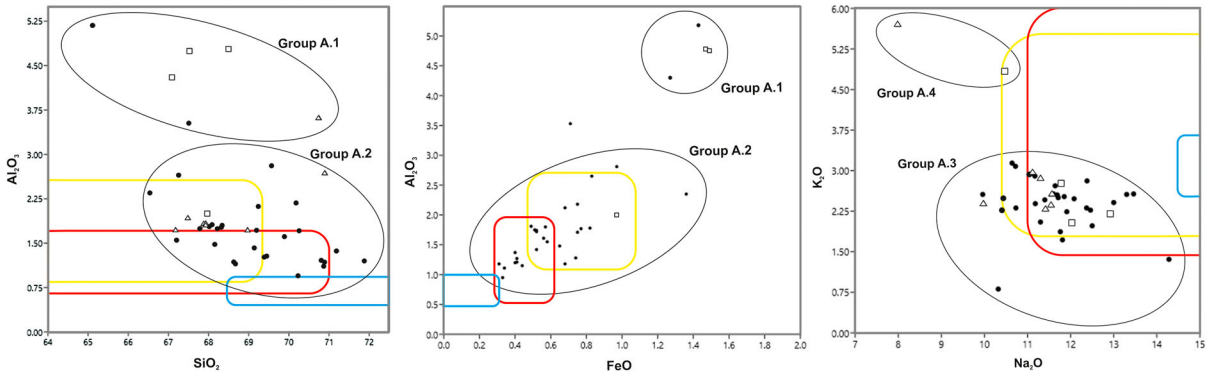

Figure 4. (a–c) Binary scatter plot diagrams, showing the compositional groups of the glass from Cucagna according to distinctive components of the raw materials. The values are given in wt.% of the oxides and were normalized to a standard base glass composition containing SiO_2, Al_2O_3, Na_2O, K_2O, CaO, MgO, FeO, MnO. The data point symbols refer to the colors of the glass fragments (black dot = colorless, "naturally" blueish, brown; triangle = blue; square = green). The biplot of Al_2O_3 vs. FeO figure (b) does not show blue glass fragments as a clear distinction between those iron oxides deriving from the coloring process with cobalt oxide and the "usual" iron impurities of the silica source is not readily possible. The colored rectangles roughly represent the maxima and minima of the three main Venetian glass types according to Verità (2013, 528, table 6.2.4) (orange = vetro commune; red = vitrum blanchum; blue = cristallo). The biplots were generated with PAST, v. 2.17, see Hammer, Harper, and Ryan (2001).

brown-purplish bottle (no. 44) and the green fragments 28, 29 and 42, as well as the blue prunted beaker (no. 39), were assumedly made of an impure sand-based silica source and the Levantine type of plant ash. The green glass sample no. 3 shows the characteristics of a glass made of pebbles and the western Mediterranean type of plant ash.

The base glass of the blue threads used for body and rim decorations of seven of the colorless samples (nos. 9, 18, 20, 23, 27, .31 and 37) is of almost equal composition as the body glass. The main colorant used to obtain the blue color is cobalt. Together with Co, traces of Ni, Cu, Zn and considerable amounts of additional iron enter the batch (see Table 4). Sample nos. 17, 19, and 36 show neither Cu and Ni or even Co, but Zn is present. The virtual absence of Co in these cases might be explainable by presuming an actual content of Co just below the detection limit of the EDAX spectrometer.

The brown to purplish color of no. 44 was obtained by a high amount of manganese (3.22%) and iron (1.40%) whereas the brown hues of no. 3 and the green color of nos. 28, 29 and 42 seem to be accidental. The high amounts of iron (0.95–1.45%) and the concurrent high amounts of manganese (1.07%–1.67%) indicate that the glassmakers may have unsuccessfully tried to eliminate the undesired coloring effect of the iron, which, on the other hand, may have entered the glass batch via an iron-rich silica source and/or as an impurity of the plant ash. Interestingly, sample no. 29 contains the same set of accompanying elements as some of the blue glass fragments (Co, Cu, Ni, Zn). This could be interpreted as an intended addition of blueish chromophores, or as an indication of recycling of blue cullet (Brems and Degryse 2014a, 133).

With respect to the contents of manganese and iron, the colorless samples may be divided in two subgroups. Overall, the iron content varies between 0.30% and 0.81%. For the first group, there are eight samples which would match the conditions of a deliberate decolorization with manganese, requiring a MnO/FeO ratio of ca. 2 (Silvestri, Molin, and Salviulo 2005, 811; Brems and Degryse 2014b, 38).

Characterization of the soil

Particle-size distribution

As displayed in Table 7 and Figure 5, the silt fraction (0.02–0.0063 mm) is predominant in most of the samples. Only sample nos. 02 and 06 show a coarser composition with sand (<0.2–0.021 mm) being the dominant component. These same samples, as well as nos. 04 and 05, contain the lowest amount of particle-sizes belonging to the clay fraction (0.0062–<0.0002 mm). Not surprisingly, there is a correlation between the texture of the soil and the location from where the soil was excavated (Figure 5). The highest amounts of clay are present in the area of the basement of Palazzo I and in the moat with its outbuildings and roads, where floors of compacted (loamy) earth can usually be expected.

Mineralogical composition

The detected minerals represent the total content of all minerals present in the bulk of the samples, regardless of the actual source. Since a certain amount of materials came in due to anthropogenic and biogenic modification of the soil, the results are to some extent uncertain. Considering calcite, it has to be taken into account that this mineral derives not only from some calcareous parent rock but also from fragments of brick, mortar or snail shells.

Minerals detected as pure compounds are quartz, calcite, kaolinite, goethite and zeolite. Other components are represented as mineralogical groups of detected species. Accordingly, K-spar comprises the

Table 4. Results of the compositional analysis of the glass from Cucagna, using an EDAX-FESEM- (UNIPV) and a WD-EPMA (KUL), the latter marked with an asterisk (*). Sample no. 27 (**) has been recuperated from scans of colorless glass of no. 26. Percentages given in wt. % of the oxides.

Sample No.	Color	Dating	Na_2O	MgO	Al_2O_3	SiO_2	P_2O_5	SO_3	Cl_2O	K_2O	CaO	TiO_2	MnO	FeO	CoO	NiO	CuO	ZnO	SnO_2	PbO
1	Colorless	14th–15th. cent.	11.63	3.55	1.19	69.71	0.14	0.41	0.98	1.69	9.75	0.05	0.52	0.40	n.d.	n.d.	n.d.	n.d.	n.d.	n.d.
2	Decolorized	14th–16th cent.	12.71	2.95	1.70	68.20	0.16	0.30	0.93	2.38	9.06	0.07	1.05	0.51	n.d.	n.d.	n.d.	n.d.	n.d.	n.d.
6	Colorless	Late Medieval	11.53	3.76	1.25	68.34	0.14	0.36	1.00	2.46	10.20	0.05	0.54	0.40	n.d.	n.d.	n.d.	n.d.	n.d.	n.d.
9	Colorless	Late Medieval	11.52	3.45	1.59	68.87	0.16	0.41	0.87	2.51	9.48	0.03	0.57	0.55	n.d.	n.d.	n.d.	n.d.	n.d.	n.d.
10	Colorless	Late Medieval	13.26	3.99	1.53	66.20	0.22	0.42	0.85	2.53	9.79	0.02	0.63	0.57	n.d.	n.d.	n.d.	n.d.	n.d.	n.d.
12	Colorless	14th–15th. cent.	11.41	3.36	1.16	69.71	0.20	0.46	0.88	2.53	9.60	0.05	0.26	0.30	n.d.	0.04	n.d.	0.05	n.d.	n.d.
14	Colorless	14th–15th. cent.	11.69	3.39	1.09	69.91	0.09	0.39	0.84	2.49	9.43	0.06	0.30	0.34	n.d.	n.d.	n.d.	n.d.	n.d.	n.d.
15	Colorless	14th cent	12.29	3.43	1.13	67.52	0.18	0.40	1.05	1.95	10.91	0.09	0.66	0.43	n.d.	n.d.	n.d.	n.d.	n.d.	n.d.
16	Colorless	14th–15th. cent.	12.18	3.05	1.68	69.10	0.23	0.27	0.91	2.76	7.75	n.d.	1.09	0.74	0.08	0.11	0.09	n.d.	n.d.	n.d.
18	Colorless	14th–15th. cent.	10.58	4.27	1.76	67.11	0.15	0.37	0.74	3.04	10.14	0.10	0.95	0.81	n.d.	n.d.	n.d.	n.d.	n.d.	n.d.
20	Decol. / blue	15th cent.	10.49	4.71	1.73	66.83	0.09	0.40	0.84	3.10	10.27	0.12	0.95	0.50	n.d.	n.d.	n.d.	n.d.	n.d.	n.d.
23	Colorless	15th cent.?	10.25	3.94	1.77	67.26	0.21	0.48	0.85	2.23	11.74	0.07	0.67	0.56	n.d.	n.d.	n.d.	n.d.	n.d.	n.d.
25	Colorless	15th cent.?	10.92	2.44	1.23	67.96	0.19	0.37	0.98	2.44	11.31	0.14	0.57	0.68	n.d.	n.d.	n.d.	n.d.	n.d.	n.d.
27**	Decol. / blue	Medieval	10.82	4.52	1.73	67.29	0.17	0.39	0.75	2.90	9.95	0.06	0.76	0.47	n.d.	0.08	n.d.	0.14	n.d.	n.d.
31	Colorless / blue	Late Medieval	12.15	4.00	1.45	66.96	0.23	0.41	1.06	2.27	9.97	0.10	0.80	0.64	n.d.	n.d.	n.d.	n.d.	n.d.	n.d.
32	Decolorized	High Medieval	11.00	4.42	1.71	67.22	0.13	0.41	0.79	2.86	9.88	0.17	0.92	0.51	n.d.	n.d.	n.d.	n.d.	n.d.	n.d.
33	Decolorized	High Medieval	10.25	2.87	3.47	66.28	0.33	0.30	1.08	2.44	10.96	0.12	1.21	0.70	n.d.	n.d.	n.d.	n.d.	n.d.	n.d.
34	Decolorized	High Medieval	11.24	3.35	1.18	70.87	0.08	0.23	1.02	2.43	8.39	0.08	0.74	0.39	n.d.	n.d.	n.d.	n.d.	n.d.	n.d.
37	Decolorized	Medieval	10.88	4.54	1.78	67.07	0.13	0.41	0.85	2.89	9.93	0.11	0.93	0.48	n.d.	n.d.	n.d.	n.d.	n.d.	n.d.
40	Decolorized	13th–15th. cent.	11.57	3.32	1.35	70.07	0.15	0.40	0.98	1.84	9.26	0.08	0.62	0.39	n.d.	n.d.	n.d.	n.d.	n.d.	n.d.
47	Colorless	Late Medieval	13.12	3.34	2.09	68.31	0.13	0.32	0.79	2.53	7.63	0.15	0.96	0.67	n.d.	n.d.	n.d.	n.d.	n.d.	n.d.
4	greenish	14th-15th cent.	11.43	3.60	1.74	67.09	0.22	0.28	0.90	2.67	10.71	0.10	0.20	0.76	0.03	0.09	0.06	0.160	n.d.	n.d.
5	Blue-greenish	Late Medieval	11.12	2.95	1.16	67.52	0.15	0.32	1.12	2.02	12.74	0.04	0.20	0.67	n.d.	n.d.	n.d.	n.d.	n.d.	n.d.
13	blueish-	14th–15th cent	9.80	3.95	2.61	66.15	0.23	0.26	0.86	2.52	12.40	0.13	0.10	0.82	n.d.	n.d.	n.d.	n.d.	n.d.	n.d.
24	greenish	15th cent.	10.12	5.08	2.30	65.26	0.35	0.07	1.37	0.79	12.99	0.18	0.21	1.33	n.d.	n.d.	n.d.	n.d.	n.d.	n.d.
41	blueish	13th–15th cent.	14.01	2.50	2.76	68.25	0.26	0.16	1.35	1.33	7.97	0.15	0.33	0.95	n.d.	n.d.	n.d.	n.d.	n.d.	n.d.
43	blueish	Medieval	11.72	3.31	1.40	68.03	0.18	0.35	1.03	2.20	10.93	0.07	0.30	0.51	n.d.	n.d.	n.d.	n.d.	n.d.	n.d.
48	blueish	15th cent.?	12.25	3.39	0.93	69.06	0.10	0.26	1.07	2.23	10.02	0.09	0.14	0.32	0.03	0.03	0.06	0.08	n.d.	n.d.
8a	Light blue	Late Medieval	11.90	3.55	1.63	69.04	n.d.	0.43	0.85	2.47	9.04	n.d.	0.55	0.54	n.d.	n.d.	n.d.	n.d.	n.d.	n.d.
8b	Dark blue	Late Medieval	11.27	3.39	1.69	67,27	n.d.	0.40	0.74	2.51	9.01	n.d.	0.59	1.80	0.37	0.30	0.66	n.d.	n.d.	n.d.
17b	Light blue	15th cent.?	10.86	4.56	1.79	67.47	n.d.	0.36	0.80	2.88	9.90	n.d.	0.91	0.47	n.d.	n.d.	n.d.	n.d.	n.d.	n.d.
17a	Dark blue	15th cent.?	11.12	4.22	1.80	66.77	n.d.	0.48	0.72	2.82	9.69	n.d.	0.90	1.05	n.d.	n.d.	n.d.	0.41	n.d.	n.d.
19b	Light blue	15th cent.	10.82	4.53	1.76	66.98	0.11	0.36	0.80	2.94	9.97	0.12	0.96	0.50	n.d.	n.d.	n.d.	0.16	n.d.	n.d.
19a	Dark blue	15th cent.	10.93	4.10	1.81	66.71	0.16	0.44	0.74	2.91	9.83	0.09	0.88	1.03	n.d.	n.d.	n.d.	0.36	n.d.	n.d.
22a	Light blue	15th cent.	10.03	3.90	1.76	67.51	n.d.	0.43	0.85	2.19	11.89	n.d.	0.68	0.55	0.03	0.10	0.09	n.d.	n.d.	n.d.
22b	Dark blue	15th cent.	9.78	3.74	1.89	66.14	n.d.	0.45	0.74	2.35	11.65	n.d.	0.71	1.74	0.22	0.14	0.48	n.d.	n.d.	n.d.
26b	Light blue	15th c.?	10.89	4.47	1.72	67.26	0.15	0.35	0.75	2.88	9.91	0.06	0.80	0.48	0.01	0.09	0.04	0.14	n.d.	n.d.
26a	Dark blue	15th c.?	10.89	4.13	1.78	66.11	0.20	0.52	0.71	2.85	9.713	0.13	0.92	1.10	0.177	0.113	0.28	0.40	n.d.	n.d.
30b	Light blue	Medieval	12.31	4.11	1.41	67.01	n.d.	0.38	1.06	2.22	10.00	n.d.	0.84	0.68	n.d.	n.d.	n.d.	n.d.	n.d.	n.d.
30a	Dark blue	Medieval	11.10	3.80	1.66	64.56	0.23	0.33	0.88	2.28	9.45	n.d.	0.82	2.43	0.59	0,76	1,14	n.d.	n.d.	n.d.
36a	Light blue	Medieval	10.90	4.22	1.76	67.24	0.17	0.36	0.85	2.83	9.99	0,10	0.92	0.52	n.d.	n.d.	n.d.	0,14	n.d.	n.d.
36b	Dark blue	Medieval	10,91	4.17	1.78	66.71	0.13	0.44	0.71	2.92	9.77	0,14	0.93	1.02	n.d.	n.d.	n.d.	0,37	n.d.	n.d.
21	Blue	End 15th c.	7.80	2.81	2.63	69.21	0.90	0.01	0.72	5.57	7.43	0,21	0.59	1.58	014	0.13	0.16	0,12	n.d.	n.d.
39	Blue	End 13th–14th c.	11.15	1.37	3.53	68.96	n.d.	0.31	1.04	2.24	7.84	0,20	0.97	1.43	0.19	0.15	0.27	0,37	n.d.	n.d.

35	Brownish	High Medieval	11.92	2.75	2.15	69.23	0.20	0.20	0.81	2.45	7.79	0,18	1.61	0.74	n.d.	n.d.	n.d.	n.d.	n.d.
44	Brown-purple	13th–14th c.	10.94	2.75	5.07	63.74	0.63	0.17	1.08	2.34	8.42	0,27	3.22	1.40	n.d.	n.d.	n.d.	n.d.	n.d.
3	Light green	14th–16th c.	10.27	2.48	1.96	66.68	0.52	0.14	1.02	4.75	9,63	0,07	1.38	0.95	n.d.	n.d.	n.d.	n.d.	0,14
28	Green	Medieval	11.83	1.46	4.7	67.37	0.17	0.12	1.10	2.01	8.46	0,28	1.07	1.45	n.d.	n.d.	n.d.	n.d.	n.d.
29	Green	Medieval	13.00	1.55	4.60	66.35	0.31	0.08	1.20	2.06	7.67	0,31	1.06	1.42	0.04	0.13	0.11	n.d.	n.d.
42	Green	13th–14th c.	11.57	1.38	4.22	65.88	0.25	0.06	1.28	2.72	9.50	0,22	1.67	1.25	n.d.	n.d.	n.d.	n.d.	n.d.
11	White opaque	Late Medieval	8.13	1.60	0.45	52.12	n.d.	n.d.	0.80	1.35	5.63	n.d.	n.d.	0.52	n.d.	n.d.	n.d.	9.49	19.90
38*	White opaque	End 13th–14th c.	6.49	1.95	1.53	52.07	0.22	0.30	0.38	1.78	5.41	0,11	0.82	0.90	0.01	n.d.	0.19	n.d.	10.33	17.51

potassium feldspars microcline and orthoclase. The group name plagioclase subsumes albite, oligoclase, andesine and anorthite. The group name of clay includes all detected three-layer clay minerals of the 2:1 structure (Velde 1992): montmorillonite, illite, smectite and chlorite. Since dolomite and ankerite are very similar in composition and structure and are often associated with each other (Anthony et al. 1995), it was not possible to make a clear distinction between both minerals with the available analytical package (sample material, diffractometer, software, database). The minerals are therefore represented as a virtual group (Table 5). The final group shown in Table 5, opal, might be misleading in interpretation. Quanta software conceives it as a group with diatomite, kerogen (both grouped by Quanta as opal A) and opal-CT, but since these siliceous and organic compounds are predominantly amorphous, they cannot be identified unambiguously with XRD (Tannenbaum et al. 1986). Assuming that the detection would be correct, kerogen could represent the amount of charcoal from destruction layers, whereas diatomite and opal-CT could be interpreted as parts of corroded glass which has already been transformed to amorphous silica and migrated into its surrounding soil matrix, e.g. by hydromechanical processes.

The predominant mineral present in the samples is quartz. Calcite and clay are also abundantly present. The amounts of clay minerals match well with the results of particle-size distribution analysis, indicating that the fractions of sand and silt are mostly composed of the remaining non-phyllosilicate minerals, mainly feldspars and quartz. This observation is in good accordance with the well-known processes of chemical weathering of feldspars (Bloemsma et al. 2012, 136). Sample no. 2009-40, deriving from the site of the destroyed Palace IV A, shows an exceptionally high amount of the group dolomite/ankerite. Sample 2009-38, taken from Moat 1, contained goethite and zeolite in small percentages (see Figure 6).

Electrochemical parameters

In view of the technical challenge to obtain stable values from the electrochemical measurements with electrodes in the eluates consisting from a solid fraction of sand and silt particles, suspended clay particles and dissolving salts in a state of establishing new equilibria, control measurements have been performed on at least two subsamples of the same parent sample. This method worked well with most of the soil samples from Cucagna, given that sufficient material could be collected (nos. 2009-38, -40, -42, -55, -56, -67; 2010-2, -3, -10, -26, -33; 2011-12, -18). As can be expected, the results of the multiple pH, Eh and EC measurements vary. The maximum standard deviations (given as percentages of the average) are 0.8% (pH), 2.9% (Eh) and 5.4% (EC). These relatively small

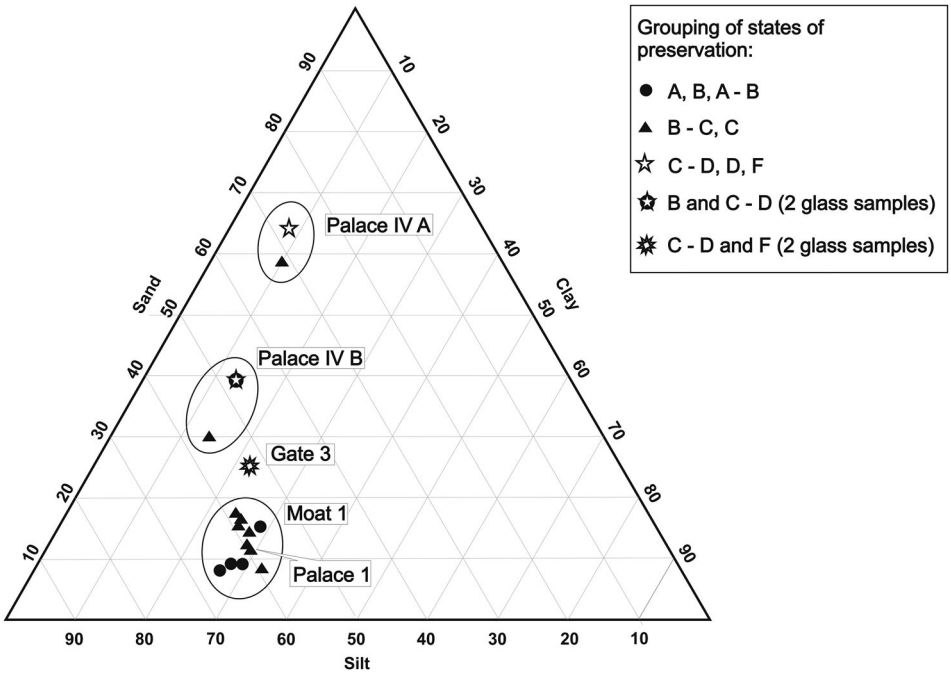

Figure 5. Ternary diagram, showing the particle-size distribution within the soil samples according to the finding place at the site of Cucagna. The data points are indicated as representations of the corresponding glass fragments and their states of preservation (see Figure 9 and Table 7). The ternary diagram was generated with TriPlot, v. 4.1.2.

Table 5. Results of the quantitative mineralogical characterization by XRD, given in weight percent.

Sample No.	Quartz	Kspar	Plag	Dol./Ank.	Kaol.	Calc	Clay	Goet	Zeol	Sylv	Opal (amorph)	∑
2009–38	45	2	5	n.d.	n.d.	2	36	1	2	1	7	100
2009–40	27	n.d.	3	35	n.d.	11	15	n.d.	n.d.	n.d.	9	100
2009–2042	33	n.d.	3	7	n.d.	28	18	n.d.	n.d.	n.d.	10	99
2009–55	17	1	3	8	n.d.	40	14	n.d.	n.d.	n.d.	17	100
2009–56	18	n.d.	3	7	n.d.	39	14	n.d.	n.d.	n.d.	19	100
2009–67	15	1	2	57	n.d.	15	6	n.d.	n.d.	n.d.	5	101
2010–02	47	n.d.	5	1	2	6	33	n.d.	n.d.	n.d.	6	100
2010–03	48	1	5	n.d.	1	7	31	n.d.	n.d.	n.d.	7	100
2010–10	38	1	6	n.d.	n.d.	5	38	n.d.	n.d.	n.d.	12	100
2010–26	48	1	5	1	n.d.	3	32	n.d.	n.d.	n.d.	10	100
2010–33	35	1	5	3	n.d.	14	32	n.d.	n.d.	n.d.	10	100
2010–38	37	1	6	2	n.d.	14	35	n.d.	n.d.	n.d.	5	100
2011–09	53	1	6	n.d.	n.d.	n.d.	37	n.d.	n.d.	n.d.	4	101
2011–11	46	1	11	n.d.	n.d.	n.d.	34	n.d.	n.d.	n.d.	8	100
2011-11a	47	3	6	n.d.	n.d.	n.d.	38	n.d.	n.d.	n.d.	5	99
2011–12	34	1	4	n.d.	n.d.	16	38	n.d.	n.d.	n.d.	7	100
2011–18	30	1	6	n.d.	n.d.	19	37	n.d.	n.d.	n.d.	7	100

Abbreviations: Kspar (potassium feldspar), Plag (plagioclase), Dol. (dolomite), Ank. (ankerite), Calc (calcite), Goet (goethite), Sylv (sylvite).

variances seem to be within tolerable ranges (cf. Husson et al. 2016 on the challenge to overcome the problem of variable Eh measurements in soils). Sample nos. 2009-38 and 2009-42 show a significantly different behavior with variances of 1.6–2.8% (pH), 11.5–13.3% (Eh) and 11.8–25.6% (EC) (see Table 6). It appears that the largest deviation occurs after reducing the amount of sub-sample material from 2 to 0.5 g. Further investigation is necessary to fully understand this phenomenon. Subject to that, it is provisionally assumed for this study that single measurements of small-sample eluates yield representative results.

The samples show very homogeneous values of hydrogen and redox potentials with slightly alkaline conditions (pH 7.65–8.18, see Tables 6 and 7). Referring to the definition of Pourbaix (1977, 4: Fig. 4), such conditions correspond with slightly reducing conditions (Figure 7). The variability of the EC measurement results (155–238 µS/cm) is higher than with pH or Eh. When compared to Eh in a binary plot diagram, there seems to be a positive trend rather than a clear positive correlation between the presence of the ions of water-soluble salts and the redox potential: increasingly oxidizing conditions imply increasing amounts of ions present in solution (Figure 8). The data are probably a consequence of mixed conditions with several half-cell reactions taking place (Böttcher and Strebel 1985, 14). The slightly alkaline milieu is probably controlled by the system $CaO–CO_2–H_2O$ (Wyllie and Tuttle 1960; Garrels and Christ 1965, 77 f.; Pollard and Heron 1996, 188). Following this assumption, there would be calcium ions (Ca^{2+}) and hydrogen carbonate

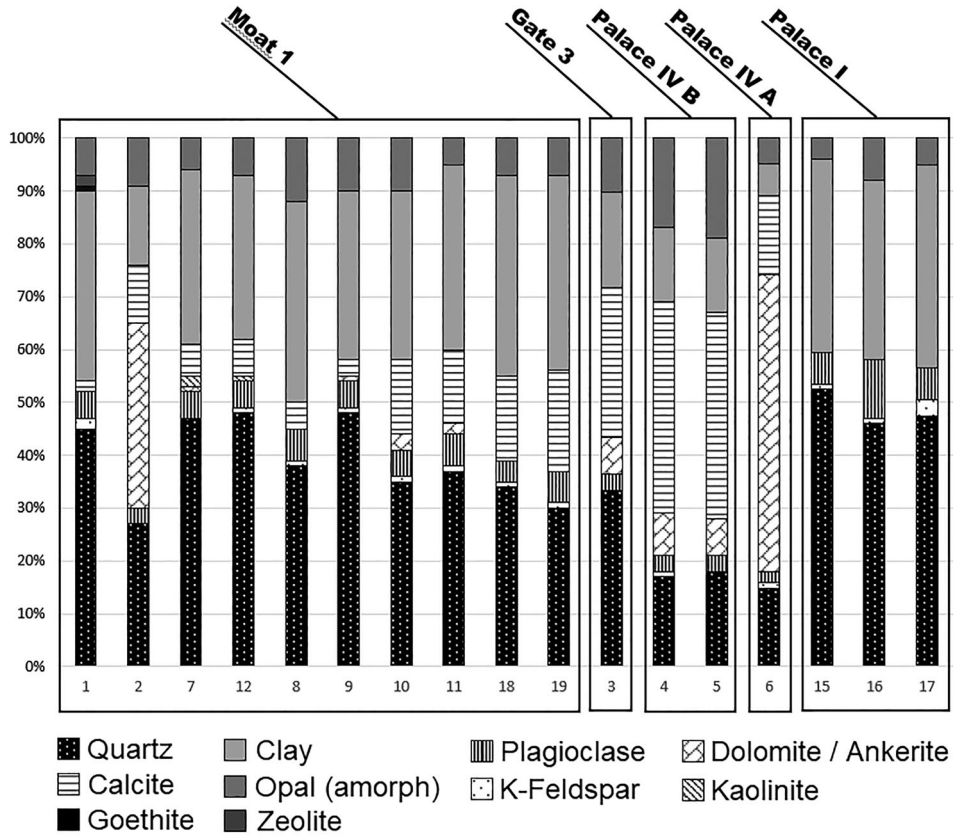

Figure 6. Stacked bar chart, showing the semi-quantitative results of the mineralogical composition analysis via XRD. The bars represent sample nos. and are grouped according to their finding place at the site of Cucagna.

Table 6. Results of control measurements for the electrochemical characterization of the soil samples from Cucagna.

Sample No.	Comment	Value	pH	EC (µS)	Eh (mV)
2009–38	4 sub-samples à	mean	7.48	225	89.5
	2 × 2 g; 2 × 0,5 g	SD	0.20	26.58	11.93
		SD (% of mean)	**2.8%**	**11.8%**	**13.3%**
2009–40	2 sub-samples à	mean	7.88	238	70
	2 g	SD	0.04	8	2
		SD (% of mean)	**0.4%**	**3.4%**	**2.9%**
2009–2042	4 sub-samples à	mean	8.15	229.7	62.5
	2 × 2 g; 2 × 0,5 g	SD	0.13	58.7	7.6
		SD (% of mean)	**1.6%**	**25.6%**	**11.5%**
2009–55	2 sub-samples à	mean	8.05	230.5	79
	2 g	SD	0.05	11.5	1
		SD (% of mean)	**0.6%**	**5.0%**	**1.3%**
2009–56	2 sub-samples à	mean	8.08	212	75
	2 g	SD	0,01	0	2
		SD (% of mean)	**0.2%**	**0%**	**2.7%**
2009–67	2 sub-samples à	mean	8.1	183	66
	2 g	SD	0.01	5	0
		SD (% of mean)	**0.1%**	**2.7%**	**0%**
2010–2	2 sub-samples à	mean	8	172.5	76
	2 g	SD	0.03	3.5	2
		SD (% of mean)	**0.3%**	**2%**	**2.6%**
2010–10	2 sub-samples à	mean	7.83	190	75.5
	2 g	SD	0.06	5	0.5
		SD (% of mean)	**0.8%**	**2.6%**	**0.7%**
2010–26	2 sub-samples à	mean	7.91	184	70
	2 g	SD	0.03	5	2
		SD (% of mean)	**0.4%**	**2.7%**	**2.9%**
2010–33	2 sub-samples à	mean	8.18	155	68.5
	2 g	SD	0.01	0	0.5
		SD (% of mean)	**0.1%**	**0%**	**0.7%**
2011–12	2 sub-samples à	mean	7.53	196.5	61.5
	1 g	SD	0.05	10.6	0.5
		SD (% of mean)	**0.7%**	**5.4%**	**0.8%**
2011–18	2 sub-samples à	mean	7.62	169.5	62
	1 g	SD	0.06	2.81	0
		SD (% of mean)	**0.7%**	**1.7%**	**0%**

Table 7. Synthesis, comparing the results of glass composition with the results of soil characterization (texture, mineralogy pH, Eh, EC).

Glass sample no. / color index	Soil sample no.	Condition	Glass composition (wt. % of oxides, displayed as elements), selected elements					Soil Texture (% of Sand, Silt, Clay)			Soil Mineralogy (%)			Soil electrochemistry (Eh in V, EC in µS)		
			Al	Na	K	Ca	Mg	Sand	Silt	Clay	Quartz	Calcite	Clay	pH	Eh	EC
39 / b *	2011-08 *	A	3.5	11.1	2.2	7.8	1.4	n.a.	n.a.	n.a.	+++	++	++	7.88	0.068	227.9
21 / b	2010-10	A-B	2.6	7.8	5.6	7.4	2.8	8.83	64.49	26.72	38	5	38	7.83	0.076	190.0
42 / g	2011-07	A-B	4.2	11.6	2.7	9.5	1.4	15.82	55.96	28.16	+++	+	++	7.80	0.076	227.9
43 / c	2011-18	A-B	1.4	11.7	2.2	10.9	3.3	9.90	62.95	27.16	30	19	37	7.62	0.062	169.5
44 / ch	2011-12	A-B	5.1	10.9	2.3	8.4	2.8	9.24	61.69	29.06	34	16	38	7.53	0.062	196.1
13 / c **	2009-55 **	B	2.6	9.8	2.5	12.4	3.9	39.65	47.19	13.15	17	40	14	8.05	0.079	230.5
16 / ch	2010-02	B-C	1.7	12.2	2.8	7.7	3.0	16.55	58.20	25.19	47	6	33	8.00	0.076	172.5
18 / c	2010-03	B-C	1.8	10.6	3.0	10.1	4.3	17.30	58.96	24.40	48	7	31	7.23	0.054	320.6
23 / c	2010-26	B-C	1.8	10.2	2.2	11.7	3.9	11.35	59.48	29.16	48	3	32	7.91	0.070	184.0
38 / w *	2011-08 *	B-C	1.5	6.5	1.8	5.4	2.0	n.a.	n.a.	n.a.	+++	++	++	7.88	0.068	227.9
41 / c	2011-09	B-C	2.8	14.3	1.4	8.1	2.6	n.a.	n.a.	n.a.	53	n.d.	37	7.91	0.085	222.7
5 / c	2009-38	C	1.2	11.3	2.1	13.0	3.0	8.78	59.04	32.21	45	2	36	7.40	0.090	225.0
14 / c	2009-56	C	1.1	11.7	2.5	9.4	3.4	29.24	55.82	14.94	18	39	14	8.08	0.075	212.0
15 / c	2009-67	C	1.1	12.3	1.9	10.9	3.4	58.63	31.06	10.26	15	15	6	8.10	0.066	183.0
25 / c	2010-38	C	1.2	11.3	2.6	10.6	3.3	12.33	59.08	28.57	37	14	35	7.91	0.056	135.1
37 / c	2011-19	C	1.8	10.9	2.9	9.9	4.5	14.92	57.86	27.21	+++	++	++	7.81	0.053	276.0
40 / c	2011-11	C	1.3	11.6	1.8	9.3	3.3	15.58	58.91	25.51	47	n.d.	34	7.49	0.077	221.2
9 / c ***	2009-2042 ***	C-D	1.5	13.3	2.5	9.8	4.0	25.60	52.06	22.34	33	28	18	8.15	0.063	229.7
6 / c	2009-40	D	1.3	11.5	2.5	10.2	3.8	63.86	27.53	8.60	27	11	15	7.88	0.070	238.0
12 / c **	2009-55 **	D	1.2	11.4	2.5	9.6	3.4	39.65	47.19	13.15	17	40	14	8.05	0.079	230.5
10 / c ***	2009-2042 ***	F	1.6	11.5	2.5	9.5	3.5	25.60	52.06	22.34	33	28	18	8.15	0.063	229.7

Notes: This table only shows those glass samples with corresponding soil samples. Entries indicated with asterisk did not have sufficient sample material available for performing the whole set of analytical approaches. In these cases, the mineralogical composition is given qualitatively. (*Index of condition:* A: very good; B: good; C: stable; D: unstable; F: substantial loss of original surface. *Color index:* c: colorless; dc: decolorized; ncb/ncg: naturally colored yellowish/blueish/greenish; ch: chestnut; b: blue; w: white). Glass samples corresponding with the same soil sample are indicated with asterisks.

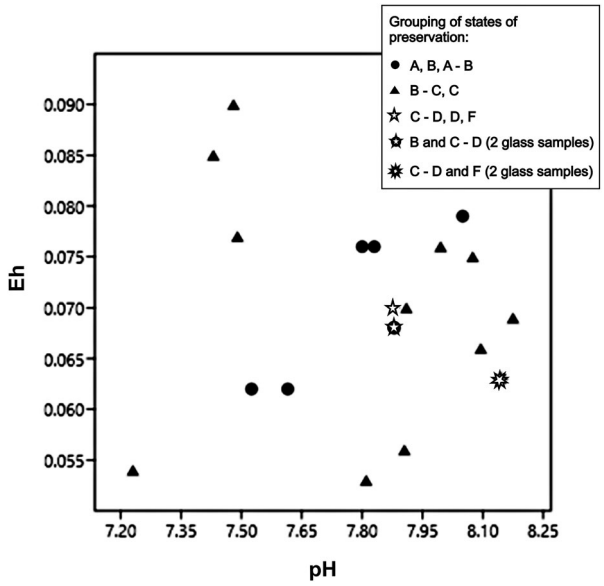

Figure 7. Plot diagram of redox potential (Eh) as a function of pH (biplot generated with PAST, v. 2.17), see Hammer, Harper, and Ryan (2001).

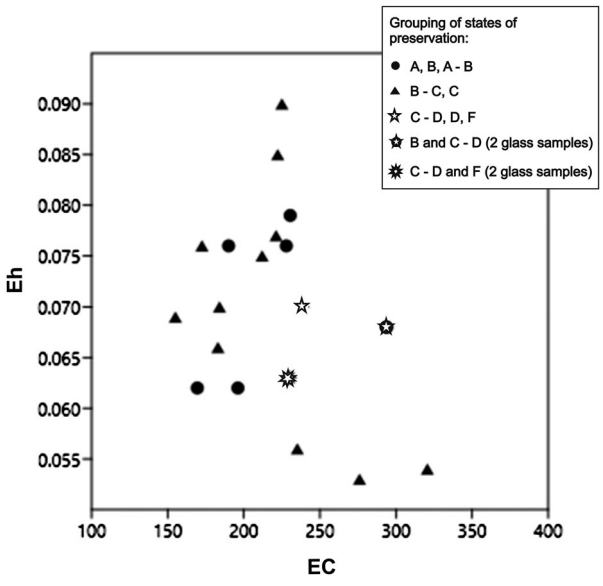

Figure 8. Plot diagram of redox potential (Eh) as a function of electrical conductivity (EC), showing a positive trend which indicates that the amount of solved components increases with rising redox potential. The state of preservation of the glass fragments seems to be not influenced by these parameters (see also Figure 7). This biplot was generated with PAST, v. 2.17, see Hammer, Harper, and Ryan (2001).

ions (HCO_3^-) present in the solution (Takeno 2005, 52 and 56). However, a detailed discussion needs to involve the results of ICP-OES with the concentrations of dissolved ions, which is still in progress.

Synthesis

According to the aim of this study, to contribute to the debate on glass corrosion under real conditions in the field, the results of the characterization of the fragments of glassware from Cucagna and their surrounding soil burial environments are put in comparison to each other. Therefore, a definition of grades of preservation is required.

Assessment of condition

According to basic principles of good practice in the conservation of archaeological finds, an attempt to

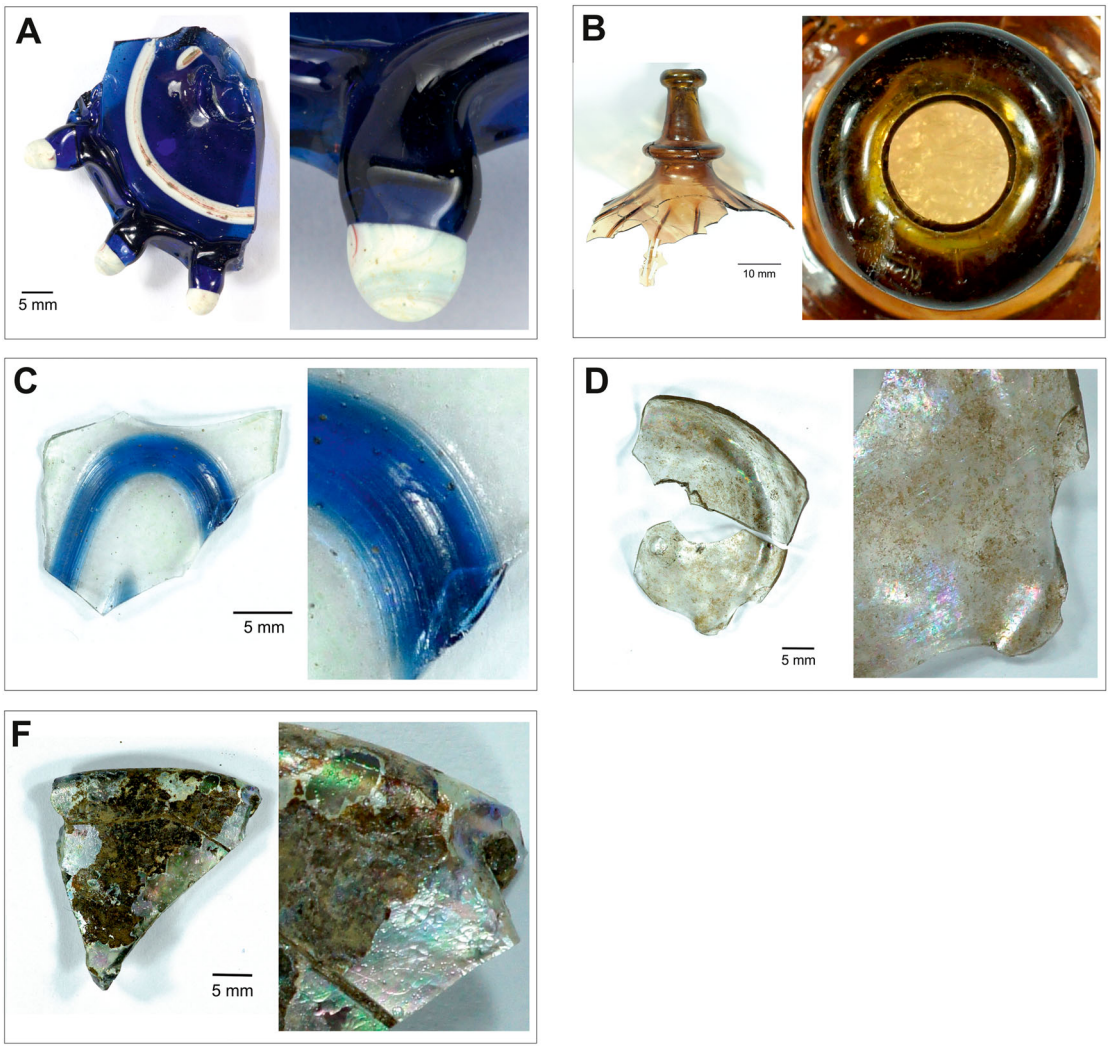

Figure 9. The five states of preservation of glass from a soil burial environment as proposed in this paper. The shown fragments refer to the following sample nos. and Cucagna catalog nos.: A: 38, 39 / 2011-065; B: 44 / 2011-161a; C: 17, 18 / 2010-011; D: 6 / 2009-258 h; F: 10 / 2009-267a. © K.T. Friedrich / IRCCZ.

assess the state of preservation should be based primarily on visual examination on macro- and microscopic scales. During the excavations of Cucagna, a simple five-step model, similar to the scheme suggested by Brill (1999a, 18), was developed and successfully applied (see Figure 9). The main criterion for assessment was the integrity of the original smooth and shining surface with possible traces of production and use. Starting from an ideal state, the model defines gradations according to the progress of leaching and alteration of the glass:

- **A**: "Very Good": The original surface remained unaltered or at least with no visible traces of corrosion.
- **B**: "Good": The original surface is still mostly present and stable, with initial stages of alteration being visible as transparent zones of iridescence or dullness.
- **C**: "Stable": The original surface is only partly (or not any more) preserved; wide zones show dullness due to the loss of thin gel layers (< 30 µm). Besides a slight roughness of the surface due to inhomogeneous pitting, striations of the glass become visible as three-dimensional relief structures on the surface.
- **D**: "Unstable": The original surface is mostly lost, or preserved within thicker (>60 µm), opaque gel layers. Zones of increased pitting and opacity are present.
- **F**: "Substantial disintegration of the glass network": No original surface is preserved. Gel layers are fragile, showing considerable thickness, opacity and iridescence at different depth zones.

Discussion

Sample nos. 13,18, 21, 24 and 44 are assessed as being in a state of very good to good preservation, with no or at least only initial traces of corrosion. Sample nos. 9, 10 and 12 are in a stable, unstable and critical state of preservation, with partially lost original surface and the formation of yellowish to dark brown, opaque zones. Sample no. 21 is a deep blue, mixed-alkali glass, with a high content of alumina. Sample nos. 10 and 18

are taken from vessels with a colorless body and blue threads (with only the body glass discussed here). Sample no. 44 belongs to an intensively brown bottle with purplish striations. The remaining fragments are from vessels of colorless glass with slight blueish, greenish or yellowish hues.

An ideal case study is provided by the sample groups of nos. 9 /10 and 12 / 13 with corresponding soil samples (Table 7). The soil formerly surrounding nos. 12 and 13 is relatively coarse, with only 13.15% of clay as a fraction of texture and 14% as a mineral group. The calcite content is quite high, possibly influencing the unfavorable, slightly alkaline milieu with pH 8.05 at moderate reducing conditions. When looking at the glass composition, it seems that the difference in alumina content is a decisive factor for the preservation of the glass (as predicted by Zachariasen 1932), whereas the content in lime is of less importance. This interpretation appears to be substantiated by the cases of the well-preserved glass sample nos. 21, 42 and 44 with high contents of alumina, and sample no. 24 showing similar contents of alumina at a relatively high pH of 8.18. Another supporting example is demonstrated by the case of nos. 38 and 39, both belonging to the fragment of a deep blue colored beaker (39) with threads of white-opaque lead glass (38). Here, the blue glass does not show any indication of leaching whereas the lead glass inlay has already lost its original glossy surface with some small, thin patches of remaining brown gel layers visible (Figures 9 and 10).

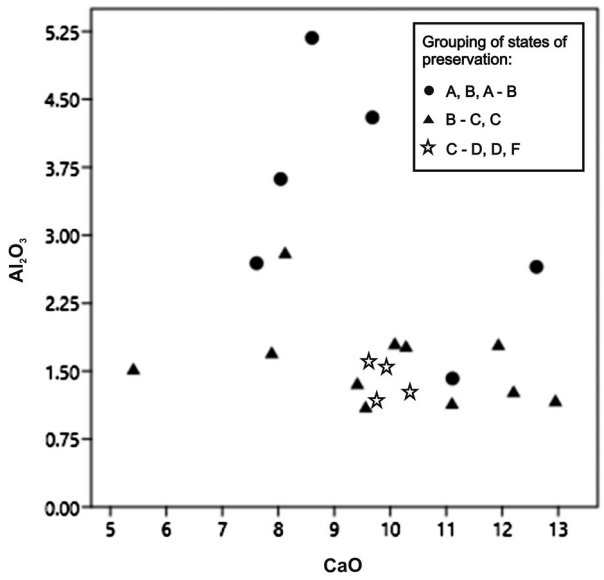

Figure 10. Binary scatter plot diagram, showing the ratio of alumina vs. lime of those glass samples with corresponding soil samples. The values are given in wt.% of the oxides and were normalized to a standard base glass composition containing SiO_2, Al_2O_3, Na_2O, K_2O, CaO, MgO, FeO, MnO. The data point symbols refer to the states of preservation (see Figure 9 and Table 7).

However, the cases of sample nos. [6 / 40] and [10 / 25] demonstrate that there are indeed more factors to consider. In both cases, the alumina contents and pH are similar: [6: Al_2O_3 1.3% / pH 7.88; 40: Al_2O_3 1.3% / pH 7.49] and [10: Al_2O_3 1.6% / 8.15; 25: $Al_2O_3$1.2% / pH 7.91], with no. 10 showing the highest percentage of Al_2O_3 in this group but the worst preservation state. Things may become more clear when looking at the particle-size and mineralogical compositions: those samples with less altered surfaces (nos. 25, 40) have been surrounded by soils with significantly higher percentages of clay as a small-size particle as well as a mineralogical component, and, at the same time, relatively low percentages of coarse-grained sand. The soils of their counterparts with more heavily corroded surfaces (nos. 6, 10) contain approx. 50% less clay minerals and 200–400% of the amount of coarse-grained sand. An explanation for this effect could be found in the swelling capacity of clay minerals of the 2:1 structure and, conversely, in the water permeability of sands. Hence, the water retention of clayey or loamy soils would be expected to be higher, theoretically leading to the establishing of more stable equilibria. The high amounts of clay minerals in the surrounding soils of sample nos. 21, 24, 43 and 44, all corresponding with relatively well-preserved or stable glass fragments, seem to support this view (see also Figure 5).

Conclusion

For this study, 44 samples of glassware from the High Medieval castle of Cucagna have been analyzed to characterize their chemical composition. According to the patterns of possible raw materials used, the glassware was probably produced in different regions of Italy, including Venice and Tuscany. At the same time, it cannot be excluded that the glass was partly imported from the Eastern Mediterranean or that it has been recycled at glass-working sites, using cullet from regions under Byzantine or Islamic patronage.

The integrated interpretation of the multi-analytical characterization of the soil burial environment has demonstrated that the evaluation of those factors influencing the preservation or deterioration of glass in the soil does not only depend on glass composition and acidity or alkalinity of the surrounding burial environment. Soil texture and mineralogical composition also have an impact, in particular when the amount of alumina as the main network stabilizing impurity in the glass is low, making the glass theoretically more prone to leaching. Hence it seems that the stability of glass in soils cannot be easily described with the characterization of only one or two parameters. A more realistic approach would be to conceive the glass fragment within its surrounding soil burial environment as a thermodynamic entity,

controlled by many interdependent parameters with variable impact on the establishment of equilibria.

Acknowledgements

The authors would like to express their gratitude for the invaluable support for the realization of the multiple analyses that needed to be conducted for this study, provided by Elvira Vassilieva, Nancy Weyns, Lore Fondu and Annelore Blomme of KU Leuven, Prof. Dr. Maria Pia Riccardi, Dr. Elena Basso and Marina Clausi of the Università degli Studi di Pavia, and Dott. Arch. Roberto Raccanello and Katharina von Stietencron of the Istituto per la Ricostruzione del Castello di Chucco-Zucco. Many thanks are given to the Soprintendenza Archaeologia, Belle Arti e Paesaggio del Friuli Venezia Giulia for granting the permission to sample and analyze the glass finds from the castle of Cucagna.

Disclosure statement

No potential conflict of interest was reported by the authors.

Notes on contributors

Karl Tobias Friedrich is head of the conservation department at the Museum of Applied Arts Cologne, Germany. His field of specialization is the conservation and restoration of siliceous materials and metals, with a focus on technological studies, conservation science and education. At KU Leuven, he is member of the Archaeometry Research Group of Prof. Degryse, currently writing his doctoral thesis.

Patrick Degryse is head of the Geology division and the Centre for Archaeological Sciences at KU Leuven and professor at both KU Leuven and Leiden University. His main research efforts focus on the use of mineral raw materials in ancient ceramic, glass, metal and building stone production, using petrographical, mineralogical and isotope geochemical techniques.

References

Anthony, J. W., R. A. Bideaux, K. W. Bladh, and M. C. Nichols. 1995. "Silica, Silicates." In *Handbook of Mineralogy*, Vol. 2 (2/2). Mineralogical Society of America, Chantilly, VA 20151-1110, USA. Accessed December 8, 2018. http://www.handbookofmineralogy.org/.

Armstrong, L. C. 1940. "Decomposition and Alteration of Feldspars and Spodumene by Water." *American Mineralogist* 25 (12): 810–820.

Barkoudah, Y., and J. Henderson. 2006. "Plant Ashes from Syria and the Manufacture of Ancient Glass: Ethnographic and Scientific Aspects." *Journal of Glass Studies* 48 (2006): 297–321.

Basso, E. 2014. "I manufatti vitrei del Castello di Cucagna (Faedis, Udine): Analisi SEM-EDS." Internal Report and Results of Compositional Analyses, received on March 14, 2014.

Basso, E., B. Messiga, and M. P. Riccardi. 2008. "Stones from Medieval Glassmaking: A Suitable Waste Product for Reconstructing an Early Stage of the Melting Process in the Mt. Lecco Glass Factory." *Archaeometry* 50 (5): 822–834.

Bianchin, S., N. Brianese, U. Casellato, F. Fenzi, P. Guerriero, P. A. Vigato, M. Battagliarin, et al. 2005b. "Medieval and Renaissance Glass Technology in Valdelsa (Florence). Part 3: Vitreous Finds and Crucibles." *Journal of Cultural Heritage* 6: 165–182.

Bianchin, S., N. Brianese, U. Casellato, F. Fenzi, P. Guerriero, P. A. Vigato, L. Nodari, U. Russo, M. Galgani, and M. Mendera. 2005a. "Medieval and Renaissance Glass Technology in Valdelsa (Florence). Part 2: Vitreous Finds and Sands." *Journal of Cultural Heritage* 6 (2005): 39–54.

Bidegaray, A.-I., A. Ceglia, M. R. Cicconi, V.-T. Pham, A. Crabbé, and E. A. Mernissi. 2018. "An in-Situ XANES Investigation of the Interactions Between Iron, Manganese and Antimony in Silicate Melts." *Journal of Non-Crystalline Solids* 502 (15): 227–235.

Biron, I., and M. Verità. 2012. "Analytical Investigation on Renaissance Venetian Enamelled Glasses from the Louvre Collections." *Journal of Archaeological Science* 39 (2012): 2706–2713.

Bloemsma, M. R., M. Zabel, J. B. W. Stuut, R. Tjallingii, J. A. Collins, and G. J. Weltje. 2012. "Modelling the Joint Variability of Grain Size and Chemical Composition in Sediments." *Sedimentary Geology* 280 (2012): 135–148.

Böhme, G. 1958. *Über die Abhängigkeit der Lauge- und Säurebeständigkeit keramischer Glasuren von deren chemischer Zusammensetzung*. Goslar: Hübener.

Böttcher, J., and O. Strebel. 1985. "Redoxpotential und Eh/pH-Diagramme von Stoffumsetzungen in reduzierendem Grundwasser (Beispiel Fuhrberger Feld)." In *Geologisches Jahrbuch Reihe C, Hydrogeologie, Ingenieurgeologie*, Heft 40, edited by Bundesanstalt für Geowissenschaften und Rohstoffe und den Geologischen Landesämtern, 3–34. Stuttgart: Schweizerbart.

Brems, D., and P. Degryse. 2014a. "Trace Element Analysis in Provenancing Roman Glass-Making." *Archaeometry* 56 (Suppl. 1): 116–136.

Brems, D., and P. Degryse. 2014b. "Western Mediterranean Sands for Glass Making." In *Glass Making in the Greco-Roman World*, edited by P. Degryse, 27–50. Leuven: Leuven University Press.

Brianese, N., U. Casellato, F. Fenzi, S. Sitran, P. A. Vigato, and M. Mendera. 2005. "Medieval and Renaissance Glass Technology in Tuscany. Part 4: The XIVth Sites of Santa Cristina (Gambassi–Firenze) and Poggio Imperiale (Siena)." *Journal of Cultural Heritage* 6 (2005): 213–225.

Brill, R. H. 1999a. *Chemical Analyses of Early Glass. Vol 1*. Corning, NY: The Corning Museum of Glass.

Brill, R. H. 1999b. *Chemical Analyses of Early Glass. Vol 2*. Corning, NY: The Corning Museum of Glass.

Cagno, S., M. Mendera, T. Jeffries, and K. Janssens. 2010. "Raw Materials for Medieval to Post-Medieval Tuscan Glassmaking: New Insight from LA-ICP-MS Analyses." *Journal of Archaeological Science* 37 (2010): 3030–3036.

Casellato, U., F. Fenzi, P. Guerriero, S. Sitran, P. A. Vigato, U. Russo, M. Galgani, M. Mendera, and A. Manasse. 2003. "Medieval and Renaissance Glass Technology in Valdelsa (Florence). Part 1: Raw Materials, Sands and non-Vitreous Finds." *Journal of Cultural Heritage* 4 (2003): 337–353.

De Bardi, M., R. Wiesinger, and M. Schreiner. 2013. "Leaching Studies of Potash-Lime-Silica Glass with Medieval Composition by IRRAS." *Journal of Non-Crystalline Solids* 360 (2013): 57–63.

De Ferri, L., D. Bersani, Ph. Colomban, P. P. Lottici, G. Simon, and G. Vezzalini. 2012. "Raman Study of Model

Glass with Medieval Compositions: Artificial Weathering and Comparison with Ancient Samples." *Journal of Raman Spectroscopy* 43 (2012): 1817–1823.

Duckworth, C. N., R. Córdoba de la Llave, E. W. Faber, D. J. Govantes Edwards, and J. Henderson. 2015. "Electron Microprobe Analysis of 9th-12th Century Islamic Glass from Córdoba, Spain." *Archaeometry* 57 (1): 27–50.

Felgenhauer-Schmiedt, S. 1995. *Die Sachkultur des Mittelalters im Lichte der Archäologischen Funde*. 2nd ed. Frankfurt: Lang.

Fenzi, F., S. Lerma, M. Mendera, B. Messiga, M. P. Riccardi, and P. A. Vigato. 2013. "Medieval Glass-Making and -Working in Tuscany and Liguria (Italy). Towards a Standard Methodology for the Classification of Glass-Making and Glass-Working Indicators." In *Modern Materials for Analysing Archaeological and Historical Glass*, edited by K. Janssens, 473–514. West Sussex: John Wiley & Sons.

Flemming, B. 2007. "The Influence of Grain-Size Analysis Methods and Sediment Mixing on Curve Shapes and Textural Parameters: Implications for Sediment Trend Analysis." *Sedimentary Geology* 202 (2007): 425–435.

Fletcher, W. W. 1972. "The Chemical Durability of Glass. A Burial Experiment at Ballidon in Derbyshire." *Journal of Glass Studies* 14 (1972): 149–151.

Friedrich, K. T. 2017. "Die Reinigung von Glas aus archäologischem Kontext: Eine Einführung." In *Handbuch der Oberflächenreinigung*, Vol. 2, 6th ed. edited by P.-B. Eipper, 90–100. Munich: Müller-Straten.

Garrels, R. M., and C. L. Christ. 1965. "Carbonate Equilibria." In *Solution, Minerals, and Equilibria*, 74–92. New York: Harper & Row.

Gasparetto, A. 1958. *Il Vetro di Murano dalle Origini ad Oggi*. Venezia: Neri Pozza Editore.

Genga, A., M. Siciliano, L. Fama, E. Filippo, T. Siciliano, A. Mangone, A. Traini, and C. Laganara. 2008. "Characterization of Surface Layers Formed under Natural Environmental Conditions on Medieval Glass from Siponto (Southern Italy)." *Materials Chemistry and Physics* 111 (2008): 480–485.

Grönwald, H. 2009. "Maria im Pantheon. Ein Pilgerzeichen von der Burg Cucagna (Friaul)." *ZAM Zeitschrift für Archäologie des Mittelalters* 37 (2009): 179–200.

Grönwald, H. 2010. "Die unterlegene eiserne Faust. Statusrelevante Metallfunde von der mittelalterlichen Burg Cucagna." *ZAM Zeitschrift für Archäologie des Mittelalters* 38 (2010): 159–204.

Hammer, Ø, D. A. T. Harper, and P. D. Ryan. 2001. "PAST: Paleontological Statistics Software Package for Education and Data Analysis." *Palaeontologia Electronica* 4 (1): 1–9. Accessed March 3, 2019. https://palaeo-electronica.org/2001_1/past/past.pdf.

Henderson, J. 2000. *The Science and Archaeology of Materials*. London: Routledge.

Husson, O., B. Husson, A. Brunet, D. Babre, K. Alary, J.-P. Sarthou, H. Charpentier, M. Durand, J. Benada, and M. Henry. 2016. "Practical Improvements in Soil Redox Potential (Eh) Measurement for Characterisation of Soil Properties. Application for Comparison of Conventional and Conservation Agriculture Cropping Systems." *Analytica Chimica Acta* 906 (2016): 98–109.

Jackson, C. M., D. Greenfield, and L. A. Howie. 2012. "An Assessment of Compositional and Morphological Changes in Model Archaeological Glasses in an Acid Burial Matrix." *Archaeometry* 54 (3): 489–507.

Jacoby, D. 1993. "Raw Materials for the Glass Industries of Venice and the Terraferma about 1370 – about 1460." *Journal of Glass Studies* 35 (1993): 65–90.

Jurek, K., and V. Hulínský. 1980. "The use and Accuracy of the ZAF Correction Procedure for the Microanalysis of Glasses." *Mikrochimica Acta* 73 (3-4): 183–198.

Lombardo, T., L. Gentaz, A. Verney-Carron, A. Chabas, C. Loisel, D. Neff, and E. Leroy. 2013. "Characterisation of Complex Alteration Layers in Medieval Glasses." *Corrosion Science* 72 (2013): 10–19.

Ludwig, U. 2009. "Zwischen Österreich, Venedig und Ungarn. Die ‚Chronik von Valvasone' als Zeugnis der Geschichte Friauls im späten Mittelalter." *Quellen und Forschungen aus italienischen Archiven und Bibliotheken* 89 (2009): 113–182.

Melcher, M., and M. Schreiner. 2005. "Evaluation Procedure for Leaching Studies on Naturally Weathered Potash-Lime-Silica Glasses with Medieval Composition By Scanning Electron Microscopy." *Journal of Non-Crystalline Solids* 351 (2005): 1210–1225.

Molchanov, V. S., and N. E. Prikhidko. 1957. "Corrosion of Silicate Glasses by Alkaline Solutions." *Bulletin of the Academy of Sciences of the USSR Division of Chemical Science* 6 (10): 1179–1184.

Monticolo, G. 1905. *I Capitolari delle Arti Veneziane sotto-poste alla Giustizia e poi alla Giustizia Vecchia dalle Origini al MDCCCXXX*. Vol. 2 (1). Rome: Istituto Storico Italiano.

Muir, E. 1993. *Mad Blood Stirring: Vendetta and Factions in Friuli During the Renaissance*. Baltimore, MD: The Johns Hopkins University Press.

Pause, C. 2000. "Late Medieval Venetian Glass." In *Annales du 14e Congrès de l'Association Internationale pour l'Histoire du Verre*, 321–325. Lochem: AIHV Association Internationale pour l'Histoire du Verre.

Pollard, M., and C. Heron. 1996. "The Chemistry, Corrosion and Provenance of Archaeological Glass." In *Archaeological Chemistry*, edited by The Royal Society of Chemistry, 149–195. Cambridge: The Royal Society of Chemistry.

Pollard, M., and C. Heron. 2008. "The Chemistry, Corrosion and Provenance of Archaeological Glass." In Chap. 5 in *Archaeological Chemistry*. 2nd ed., edited by The Royal Society of Chemistry, 144–192. Cambridge: The Royal Society of Chemistry.

Pourbaix, M. 1977. "Electrochemical Corrosion and Reduction." In *Corrosion and Metal Artifacts – A Dialogue Between Conservators and Corrosion Scientists*. Vol. 479., edited by F. Brown, H. C. Burnett, W. T. Chase, M. Goodway, J. Kruger, and M. Pourbaix, 1–16. Gaithersburg, MD: U.S. Department of Commerce / National Bureau of Standards: NBS Special Publication.

Quartieri, S., M. P. Riccardi, B. Messiga, and F. Boscherini. 2005. "The Ancient Glass Production of the Medieval Val Gargassa Glasshouse: FE and Mn XANES Study." *Journal of Non-Crystalline Solids* 351 (2005): 3013–3022.

Raman, C. V., and V. S. Rajagopalan. 1939. "The Structure and Optical Characters of Iridescent Glass." *Proceedings of the Indian Academy of Sciences - Section A* 9 (1939): 371–381.

Salviulo, G., A. Silvestri, G. Molin, and R. Bertoncello. 2004. "An Archaeometric Study of the Bulk and Surface Weathering Characteristics of Early Medieval (5th–7th Century) Glass From the Po Valley, Northern Italy." *Journal of Archaeological Science* 31 (2004): 295–306.

Schalm, O., D. Caluwé, H. Wouters, K. Janssens, F. Verhaeghe, and M. Pieters. 2004. "Chemical Composition and Deterioration of Glass Excavated in the 15th–16th Century Fishermen Town of Raversijde (Belgium)." *Spectrochimica Acta Part B: Atomic Spectroscopy* 59 (2004): 1647–1656.

Schalm, O., K. Proost, K. De Vis, S. Cagno, K. Janssens, F. Mees, P. Jacobs, and J. Caen. 2011. "Manganese Staining of Archaeological Glass: The Characterization of Mn-Rich Inclusions in Leached Layers and a Hypothesis of its Formation." *Archaeometry* 53 (1): 103–122.

Silvestri, A., G. Molin, and G. Salviulo. 2005. "Roman and Medieval Glass from the Italian Area: Bulk Characterization and Relationships with Production Technologies." *Archaeometry* 47 (4): 797–816.

Smets, B., and T. Lommen. 1982. "The Leaching of Sodium Containing Glasses: Ion Exchange or Diffusion of Molecular Water?" *Journal de Physique Colloques* 43 (C9): 649–652.

Takeno, N. 2005. *Atlas of Eh-pH-Diagrams: Intercomparison of Thermodynamic Databases*. Geological Survey of Japan Open File Report No. 419. Tokyo: National Institute of Advanced Industrial Science and Technology, Research Center for Deep Geological Environments.

Tannenbaum, E., E. Ruth, B. J. Huizinga, and I. R. Kaplan. 1986. "Biological Marker Distribution in Coexisting Kerogen, Bitumen and Asphaltenes in Monterey Formation Diatomite, California." *Organic Geochemistry* 10: 531–536.

Tite, M. S., A. Shortland, Y. Maniatis, D. Kavoussanaki, and S. A. Harris. 2006. "The Composition of the Soda-Rich and Mixed Alkali Plant Ashes Used in the Production of Glass." *Journal of Archaeological Science* 33 (2006): 1284–1292.

Velde, B. 1992. *Introduction to Clay Minerals: Chemistry, Origins, Uses and Environmental Significance*. London: Chapman & Hall.

Velde, B. 2013. "Glass Compositions Over Several Millennia in the Western World." In *Modern Materials for Analysing Archaeological and Historical Glass*, edited by K. Janssens, 67–78. West Sussex: John Wiley & Sons.

Verità, M. 1985. "L'invenzione del Cristallo Muranese: Una Verifica Analitica dell Fonti Storiche." *Rivista della Stazione Sperimentale del Vetro* 15 (1985): 17–29.

Verità, M. 1995. "Analytical Investigation of European Enameled Beakers of the 13th and 14th Centuries." *Journal of Glass Studies* 37 (1995): 83–98.

Verità, M. 2013. "Venetian Soda Glass." In *Modern Materials for Analysing Archaeological and Historical Glass*, edited by K. Janssens, 515–536. West Sussex: John Wiley & Sons.

Verità, M., A. Renier, and S. Zecchin. 2002. "Chemical Analyses of Ancient Glass Findings Excavated in the Venetian Lagoon." *Journal of Cultural Heritage* 3 (2002): 261–271.

Vicenzi, E. P., S. Eggins, A. Logan, and R. Wysoczanski. 2002. "Microbeam Characterization of Corning Archeological Reference Glasses: New Additions to the Smithsonian Microbeam Standard Collection." *Journal of Research of the National Institute of Standards and Technology* 107 (6): 719–727.

Vranová, V., Th Danso Marfo, and K. Rejšek. 2015. "Soil Scientific Research Methods used in Archaeology - Promising Soil Biochemistry: A Mini Review." *Acta Universitatis Agriculturae et Silviculurae Mendelianae Brunensis* 63 (4): 1417–1426.

Warren, B. E. 1934. "The Diffraction of X-Rays in Glass." *Physical Review* 45 (10): 657–661.

Watkinson, D., L. Weber, and K. Anheuser. 2005. "Staining of Archaeological Glass from Manganese-Rich Environments." *Archaeometry* 47 (1): 69–82.

Wedepohl, K. H. 2003. *Glas in Antike und Mittelalter: Geschichte eines Werkstoffs*. Stuttgart: Schweizerbart.

Wedepohl, K. H., and K. Simon. 2010. "The Chemical Composition of Medieval Wood Ash Glass from Central Europe." *Geochemistry* 70 (2010): 89–97.

Weltje, G. J., and H. von Eynatten. 2004. "Quantitative Provenance Analysis of Sediments: Review and Outlook." *Sedimentary Geology* 171 (2004): 1–11.

Weyns, N. 2017. Internal Report, July 28, 2017. KU Leuven, Faculty of Science, Geo-Institute, Department of Earth and Environmental Science.

Wyllie, P. J., and O. F. Tuttle. 1960. "The System CaO-CO_2-H_2O and the Origin of Carbonatites." *Journal of Petrology* 1 (1): 1–46.

Zachariasen, F. W. H. 1932. "The Atomic Arrangement in Glass." *Journal of the American Ceramic Society* 54 (10): 3841–3851.

Zoleo, A., M. Brustolon, A. Barbon, A. Silvestri, G. Molin, and S. Tonietto. 2015. "Fe(III) and Mn(II) EPR Quantitation in Glass Fragments From the Palaeo-Christian Mosaic of St. Prosdocimus (Padova, NE Italy): Archaeometric and Colour Correlations." *Journal of Cultural Heritage* 16: 322–328.